

The separate-universe approach and sudden transitions during inflation

Joseph H. P. Jackson,^a Hooshyar Assadullahi,^{a,b} Andrew D. Gow,^a Kazuya Koyama,^a Vincent Vennin,^{c,a} David Wands^a

^aInstitute of Cosmology & Gravitation, University of Portsmouth, Dennis Sciamia Building, Burnaby Road, Portsmouth, PO1 3FX, United Kingdom

^bSchool of Mathematics and Physics, University of Portsmouth, Lion Gate Building, Lion Terrace, Portsmouth, PO1 3HF, United Kingdom

^cLaboratoire de Physique de l'École Normale Supérieure, ENS, CNRS, Université PSL, Sorbonne Université, Université Paris Cité, F-75005 Paris, France

E-mail: joseph.jackson@port.ac.uk, hooshyar.assadullahi@port.ac.uk,
andrew.gow@port.ac.uk, kazuya.koyama@port.ac.uk, vincent.vennin@ens.fr,
david.wands@port.ac.uk

Abstract. The separate-universe approach gives an intuitive way to understand the evolution of cosmological perturbations in the long-wavelength limit. It uses solutions of the spatially-homogeneous equations of motion to model the evolution of the inhomogeneous universe on large scales. We show that the separate-universe approach fails on a finite range of super-Hubble scales at a sudden transition from slow roll to ultra-slow roll during inflation in the very early universe. Such transitions are a feature of inflation models giving a large enhancement in the primordial power spectrum on small scales, necessary to produce primordial black holes after inflation. We show that the separate-universe approach still works in a piece-wise fashion, before and after the transition, but spatial gradients on finite scales require a discontinuity in the homogeneous solution at the transition. We discuss the implications for the δN formalism and stochastic inflation, which employ the separate-universe approximation.

Keywords: Cosmological perturbation theory, inflation, physics of the early universe, primordial black holes

Contents

1	Introduction	1
2	Separate-universe approach	3
2.1	Homogeneous background	3
2.2	Linear perturbations	4
2.3	Separate-universe approach	6
2.3.1	k^2 -expansion	6
2.4	Super-Hubble matching	9
2.4.1	Homogeneous matching	9
2.4.2	Matching including k^2 -corrections	9
2.4.3	The δN formalism	10
3	Piece-wise linear potential	11
3.1	Homogeneous background	11
3.2	Perturbations	12
3.3	Homogeneous matching	15
3.4	Including k^2 -corrections	18
4	Smooth potential with a Gaussian bump	19
5	Implications for stochastic inflation	21
6	Conclusion	22
A	δN for piece-wise linear model	24
B	Example: inflection-point model	28
C	Bessel functions	29

1 Introduction

Inflation is a period of rapid, accelerated expansion in the very early universe [1–6], which explains a number of observational properties of our universe, including the origin of large-scale structure. Initial quantum field fluctuations, $\delta\phi$, are expanded to from small to super-Hubble scales by the accelerated expansion [7–12], where they give rise to primordial curvature perturbations, \mathcal{R} [13, 14]. The almost scale-invariant power spectrum of large-scale perturbations, $\mathcal{P}_{\mathcal{R}}$, predicted by canonical slow-roll inflation using linear perturbation theory is in excellent agreement with observations of the cosmic microwave background (CMB) [15–17].

We are yet to directly observe the primordial power spectrum on smaller scales, which left the Hubble radius closer to the end of inflation. A large enhancement of the perturbations compared to those observed on CMB scales would be required in order to produce observable signals [18], such as a stochastic gravitational-wave background [19, 20] or primordial black holes (PBHs) [21]. The former has been highlighted by the recent pulsar timing array detection of a stochastic gravitational-wave background [22–24], which could be of primordial origin [25]. The latter is of particular interest to explain some or all of the dark matter in our universe [26–29].

To produce a large enhancement in the power spectrum, the usual slow-roll behaviour needs to be interrupted, typically with a period of ultra-slow-roll (USR) inflation [30, 31]. As this requires breaking away from the slow-roll attractor solution, a localised feature in the potential is needed [32], which induces a sudden transition. The transition produces a large effective mass-squared for a limited time period in the Sasaki–Mukhanov mode equation [33, 34]. The enhanced power spectrum can also amplify non-linearities in \mathcal{R} . This gives the possibility of loop corrections to the power spectrum dominating over the tree-level result on large scales [35–43], potentially leading to a breakdown of the perturbative framework.

One approach which enables us to go beyond a purely perturbative description is the δN formalism [9, 44–47]. Here we identify the primordial curvature perturbation, \mathcal{R} , with δN , the difference between $N(\phi + \delta\phi)$, the local integrated logarithmic expansion (or e-folds) from an initial spatially-flat hypersurface to the end of inflation hypersurface, and its mean value $N(\phi)$, *i.e.*

$$\delta N = N(\phi + \delta\phi) - N(\phi). \quad (1.1)$$

It is possible to treat long-wavelength (typically, super-Hubble scale) fluctuations as classical perturbations of a homogeneous and isotropic cosmology – the so-called separate-universe approach [48–51]. The homogeneous perturbation can be obtained as the long-wavelength limit in a gradient expansion [52, 53]. This enables us to find the local integrated expansion, $N(\phi + \delta\phi)$, using the fully non-linear equations of General Relativity for a homogeneous and isotropic cosmology, evolving the local fields and expansion rate, while neglecting spatial gradients. In the classical δN approach we use the classical solutions for $N(\phi)$ to obtain δN from Eq. (1.1), which can give a highly non-Gaussian probability distribution for δN [54–58], even starting from Gaussian field perturbations, $\delta\phi$. In the stochastic δN approach [59–61] we also include the cumulative effect of quantum field fluctuations all along the trajectory, leading to a stochastic description for $\mathcal{N}(\phi)$, where \mathcal{N} now indicates a stochastic variable.

However, we will show that a sudden transition from slow-roll to ultra-slow-roll evolution during inflation leads to non-adiabatic behaviour. This gives rise to particle production on sub-Hubble scales and non-adiabatic perturbations on super-Hubble scales, sourced by gradient terms [62]. While the separate-universe description applies both before and after the transition, the key role played by gradient terms implies that the naïve separate-universe approach breaks down at the transition itself. This necessitates a re-appraisal of how we apply the classical and stochastic δN formalisms.

In this paper we first introduce the mathematical framework to identify the long-wavelength limit of the perturbed fields, which we refer to as homogeneous solutions, and then discuss their use in the separate-universe approach in Sec. 2. In Sec. 3 we study the behaviour of the homogeneous perturbations in a simple model of an instantaneous transition using the piece-wise linear potential of Starobinsky [63]. Here, there is a non-adiabatic transition from slow roll to ultra-slow roll, followed by an adiabatic transition back to slow roll. Using analytical and numerical solutions, we explicitly show that the sudden transition leads to discontinuities in the homogeneous solutions, sourced by gradient terms at the transition. We then demonstrate in Sec. 4 that the same behaviour is seen in an example of a smooth potential with a localised feature, which induces a single sudden transition, using numerical methods to find the homogeneous component of the perturbation post-transition. Finally, we discuss in Sec. 5 how the stochastic δN approach might be modified to account for non-adiabatic effects in homogeneous perturbations at a transition from slow roll to ultra-slow roll. We conclude in Sec. 6. Supporting calculations and another example of a single and sudden transition in a smooth potential are presented in the appendices. Throughout we work in natural units in which $c = \hbar = 8\pi G = 1$.

2 Separate-universe approach

2.1 Homogeneous background

The background dynamics of inflation driven by a spatially-homogeneous canonical single scalar field, $\phi(t)$, with potential energy $V(\phi)$, in a homogeneous and isotropic spacetime with scale factor $a(t)$, are given by the Klein–Gordon equation

$$\ddot{\phi} + 3H\dot{\phi} + \frac{dV(\phi)}{d\phi} = 0, \quad (2.1)$$

where an over-dot denotes a derivative with respect to cosmic time, t . The Hubble expansion rate, $H = \dot{a}/a$, is given by the Friedmann equation

$$3H^2 = V(\phi) + \frac{1}{2}\dot{\phi}^2. \quad (2.2)$$

The inflationary expansion can be described by the Hubble-flow parameters [64, 65]

$$\epsilon_{i+1} = \frac{d \ln \epsilon_i}{dN}, \quad \epsilon_0 = \frac{H_{\text{in}}}{H}, \quad (2.3)$$

where H_{in} is the Hubble expansion rate at some initial time. Inflation occurs whenever $\epsilon_1 < 1$. Slow-roll inflation requires $|\epsilon_i| \ll 1 \ \forall i \geq 1$, corresponding to $\ddot{\phi}$ being subdominant in Eq. (2.1). The ultra-slow-roll limit of inflation requires $\epsilon_1 \ll 1$ and $\epsilon_2 \simeq -6$, corresponding to $dV(\phi)/d\phi$ being subdominant in Eq. (2.1) [66]. Typically, ultra-slow roll corresponds to a transient phase, followed by a return to a slow-roll (or constant-roll) attractor [67]. Since slow roll is always an attractor whenever it exists, a deviation from the slow-roll attractor requires a feature in the potential, causing a sudden transition to ultra-slow roll.

2.2 Linear perturbations

Inhomogeneous perturbations about the homogeneous and isotropic background can be described by the Sasaki–Mukhanov variable [33, 34], $v \equiv a\delta\phi$, where $\delta\phi(t, \vec{x})$ corresponds to scalar field perturbations in the spatially-flat gauge [68].

Linear perturbations can be decomposed into independent wavemodes, v_k , with comoving wavenumber, k , which obey the Sasaki–Mukhanov mode equation [33, 34]

$$v_k'' + (k^2 + \mu^2)v_k = 0, \quad (2.4)$$

where a prime denotes a derivative with respect to comoving time, $\eta \equiv \int dt/a$, and $\mu^2 \equiv -z''/z$, where we define $z = a\dot{\phi}/H = \text{sign}(\dot{\phi})\sqrt{2a^2\epsilon_1}$. The time-dependent mass-squared term in Eq. (2.4) can be written in terms of the Hubble-flow parameters (2.3) as

$$\mu^2 = (aH)^2 \left(-2 + \epsilon_1 - \frac{3}{2}\epsilon_2 + \frac{1}{2}\epsilon_1\epsilon_2 - \frac{1}{4}\epsilon_2^2 - \frac{1}{2}\epsilon_2\epsilon_3 \right). \quad (2.5)$$

If we assume that the scalar field starts in the Bunch–Davies vacuum state on small scales during inflation ($k^2 \gg |\mu^2|$) then this sets the initial condition for the mode function

$$v_k^{\text{BD}} = \frac{e^{-ik\eta}}{\sqrt{2k}}. \quad (2.6)$$

In our numerical solutions we will assume that each mode v_k is in the Bunch–Davies vacuum state at an initial time $-k\eta_{\text{in}} = 10^3$. The subsequent evolution for a given mode is then given by Eq. (2.4) and depends solely on the time-dependence of μ^2 given by Eq. (2.5).

Note that so far we have placed no restriction on the values that the Hubble-flow parameters may take in Eq. (2.5). We will consider models of inflation with a localised feature in the potential causing a sudden transition to ultra-slow roll, coinciding with a large mass-squared, $\mu^2 > (aH)^2$, in Eq. (2.5). This behaviour is illustrated in Fig. 1 for three specific inflation models which we will investigate in this paper. We will define a sudden transition to be a period of less than one e-fold ($\Delta N \lesssim 1$) where μ^2 is large and positive.

In addition to the Sasaki–Mukhanov variable, v , we will be interested in the comoving curvature perturbation, $\mathcal{R} = v/z$ [68]. For general matter content, with density ρ and pressure P , the time-dependence of \mathcal{R} is given by

$$\dot{\mathcal{R}} = \frac{H}{\rho + P} \delta P_{\text{com}}, \quad (2.7)$$

where the comoving pressure perturbation can be split into adiabatic and non-adiabatic components, $\delta P_{\text{com}} = c_s^2 \delta \rho_{\text{com}} + \delta P_{\text{nad}}$, and $c_s^2 = \dot{P}/\dot{\rho}$ is the adiabatic sound speed. The comoving density perturbation is related via the Einstein constraint equations to the divergence of the Bardeen metric potential [68] and thus the time-dependence of \mathcal{R} can be written as

$$\dot{\mathcal{R}} = \frac{H}{\rho + P} \left(\frac{2c_s^2}{a^2} \nabla^2 \Psi + \delta P_{\text{nad}} \right). \quad (2.8)$$

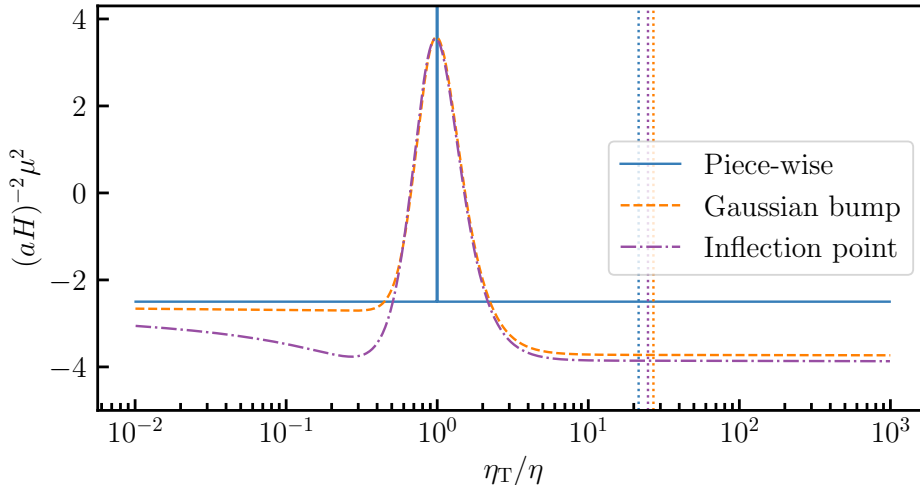


Figure 1. The evolution of the effective mass-squared, μ^2 , in the Sasaki–Mukhanov mode equation (2.5) relative to the comoving Hubble rate, near a sudden transition in the three inflation models investigated in this paper. The piece-wise linear potential is studied in Sec. 3, the Gaussian bump model in Sec. 4 and the inflection-point model in Appendix B. For each potential the transition time, η_T , is defined to be the first time for which $\epsilon_2 < -3$. The dotted vertical lines indicate the time when ultra-slow roll ends, defined to be when $\epsilon_2 > -3$. The similarity in the behaviour of μ^2 close to its maximum is due to model parameters being tuned to produce a PBH abundance consistent with PBHs being all of the dark matter.

Therefore, in the absence of non-adiabatic pressure perturbations ($\delta P_{\text{nad}} = 0$), the comoving curvature is constant on sufficiently large scales where we can neglect spatial gradients of the Bardeen potential $\nabla^2 \Psi \rightarrow 0$ [69]. This makes \mathcal{R} convenient to track the evolution of adiabatic density perturbations on large scales during inflation, and through the end of inflation, as the inflaton energy is transferred to the particles of the standard model, reheating the primordial universe [70, 71].

During single-field inflation the comoving density perturbation in the scalar field can also be related to the non-adiabatic pressure perturbation [72] and, noting that the adiabatic sound speed for a single field is given by $c_s^2 = 1 - (2V'/3H\dot{\phi})$, we find¹

$$\dot{\mathcal{R}} = -\frac{3H^2}{2\dot{V}}\delta P_{\text{nad}}. \quad (2.9)$$

Thus the time-dependence of \mathcal{R} is directly determined by the non-adiabatic part of the scalar field’s pressure perturbation on all scales. In the following we shall show that the non-adiabatic pressure perturbation does not vanish on all super-Hubble scales after a sudden transition from slow roll to ultra-slow roll.

¹See Ref. [73] for a general discussion of the time-dependence of the comoving curvature perturbation.

2.3 Separate-universe approach

One might expect that the evolution of inhomogeneous scalar field perturbations on sufficiently long wavelengths, where spatial gradients become negligible, can be described locally by spatially-homogeneous perturbations of the background Klein–Gordon equation (2.1). This is the separate-universe approach [46–48] commonly used to simplify the study of inhomogeneous perturbations on large scales.

Considering a small *homogeneous* perturbation about the background scalar field, $\phi \rightarrow \phi(t) + \delta\phi_h(t)$, and about the background spacetime (specifically perturbing the Hubble rate, $H \rightarrow H + \delta H$ given by (2.2), and the lapse function relating cosmic time to proper time, $dt \rightarrow (1 + A)dt$), one obtains a linear equation for the homogeneous scalar field perturbation [74]

$$\delta\ddot{\phi}_h + 3H\delta\dot{\phi}_h + \left[\frac{d^2V}{d\phi^2} - a^{-3} \frac{d}{dt} \left(\frac{a^3 \dot{\phi}^2}{H} \right) \right] \delta\phi_h = 0. \quad (2.10)$$

One can verify [74] that this is equivalent to setting $k \rightarrow 0$ in the Sasaki–Mukhanov mode equation (2.4) for $v_h = a\delta\phi_h$:

$$v_h'' + \mu^2 v_h = 0. \quad (2.11)$$

From the form of the inhomogeneous mode equation (2.4) we would expect this to be a good approximation on sufficiently large scales ($k^2 \ll |\mu^2|$).

The general solution for corresponding homogeneous curvature perturbation, $\mathcal{R}_h = v_h/z$, is given by

$$\mathcal{R}_h = C + D \int_{\eta}^{\eta_1} \frac{d\tilde{\eta}}{z^2(\tilde{\eta})}, \quad (2.12)$$

where C and D are constants of integration. C corresponds to the curvature perturbation at $\eta = \eta_1$, while D determines the amplitude of the isocurvature perturbation at η_1 . More generally D can be identified with a non-adiabatic homogeneous perturbation since it controls $\dot{\mathcal{R}}_h$, see Eq. (2.9).

The choice of η_1 in (2.12) is arbitrary and is degenerate with C . If we set η_1 to be the end of inflation, which we take to be $\eta_1 = 0$, then the two terms appearing in Eq. (2.12) can be identified as the homogeneous growing and decaying modes. The growing mode is in fact constant, while the decaying mode decreases in slow roll where $1/z^2 \propto \eta^2$ and increases in ultra-slow roll where $1/z^2 \propto \eta^{-4}$. It vanishes at the end of inflation by construction.

2.3.1 k^2 -expansion

One can include systematic corrections to the homogeneous solution by performing an expansion of the Sasaki–Mukhanov equation (2.4) in k^2 . To that end, it is convenient to first write down the equation of motion for $\mathcal{R}_k = v_k/z$ that follows from Eq. (2.4), namely

$$\mathcal{R}_k'' + 2\frac{z'}{z}\mathcal{R}_k' + k^2\mathcal{R}_k = 0. \quad (2.13)$$

For any finite k the decomposition into growing and decaying modes, $\mathcal{R}_k = \mathcal{G} + \mathcal{D}$, where \mathcal{G} and \mathcal{D} are themselves solutions of Eq. (2.13), can be carried out order-by-order in k^2 , by expanding

$$\mathcal{G}(\eta) = \sum_n \mathcal{G}_n(\eta) k^{2n} \quad \text{and} \quad \mathcal{D}(\eta) = \sum_n \mathcal{D}_n(\eta) k^{2n}. \quad (2.14)$$

At leading order in k^2 for a given wavemode we recover the homogeneous behaviour (2.12)

$$\mathcal{G}_0 \equiv C_k \quad \text{and} \quad \mathcal{D}_0(\eta) \equiv D_k \int_{\eta}^0 \frac{d\tilde{\eta}}{z^2(\tilde{\eta})}. \quad (2.15)$$

By identifying terms of the same order in k^2 in Eq. (2.13), one finds

$$\mathcal{G}_n'' + 2\frac{z'}{z}\mathcal{G}_n' = -\mathcal{G}_{n-1}, \quad (2.16)$$

which leads to the recursive solution for the growing mode

$$\mathcal{G}_n(\eta) = \int_{\eta}^{\eta_3} \frac{d\tilde{\eta}}{z^2(\tilde{\eta})} \int_{\eta_2}^{\tilde{\eta}} d\tilde{\eta} z^2(\tilde{\eta}) \mathcal{G}_{n-1}(\tilde{\eta}), \quad (2.17)$$

with a similar expression for the decaying mode, $\mathcal{D}_n(\eta)$.

Two arbitrary integration limits have to be introduced, η_2 and η_3 . We will require that the k^2 -corrections vanish at the end of inflation at all orders in k , which sets $\eta_3 = 0$ in \mathcal{G}_n , and we further impose that $\eta_3 = 0$ in \mathcal{D}_n as well, such that at the end of inflation the value of \mathcal{R}_k corresponds to C_k and the power spectrum of the curvature perturbation reads

$$\mathcal{P}_{\mathcal{R}}(k) = \frac{k^3}{2\pi^2} |C_k|^2. \quad (2.18)$$

There is no unique prescription for η_2 . In practice, one notices that changing η_2 in Eq. (2.17) adds a contribution proportional to \mathcal{D}_0 into \mathcal{G}_n and \mathcal{D}_n . In particular, the k^2 -correction to the growing mode, $\mathcal{G}_1(\eta)$, is only defined up to terms proportional to the leading-order decaying mode, $\mathcal{D}_0(\eta)$ [62].

Solution for massless inflaton field in de Sitter

In order to illustrate how the k^2 -expansion works, let us consider the simple limit of a massless inflaton field in de Sitter, corresponding to $\epsilon_1 \rightarrow 0$, such that H is a constant and $a = -1/(H\eta)$, and $\mu^2 \Rightarrow -2/\eta^2$ in Eq. (2.5). This holds in both the slow-roll limit ($\epsilon_i \rightarrow 0$ for all $i \geq 1$) or the ultra-slow-roll limit ($\epsilon_1 \rightarrow 0$, $\epsilon_2 \rightarrow -6$, and $\epsilon_i \rightarrow 0$ for all $i \geq 3$). In this case Eq. (2.13) can be solved analytically

$$\mathcal{R}_k = \frac{\text{sign}(\dot{\phi})}{2a\sqrt{k\epsilon_1}} \left[\alpha_k \left(1 - \frac{i}{k\eta} \right) e^{-ik\eta} + \beta_k \left(1 + \frac{i}{k\eta} \right) e^{ik\eta} \right]. \quad (2.19)$$

where the integration constants α_k and β_k are Bogoliubov coefficients. In the Bunch–Davies vacuum (2.6), $\alpha_k = 1$ and $\beta_k = 0$ but we will keep them general for now.

Let us perform the k^2 -expansion in the slow-roll limit where ϵ_1 can be considered to be a constant. First, from Eq. (2.15), one has $\mathcal{G}_0 = C_k$ and $\mathcal{D}_0 = -D_k H^2 \eta^3 / (6\epsilon_1)$. Then, for the growing mode, one can show that the ansatz $\mathcal{G}_n = C_k g_n \eta^{2n}$ satisfies Eq. (2.17) if

$$g_n = -\frac{g_{n-1}}{2n(2n-3)}. \quad (2.20)$$

Note that in order to get this expression, we must set η_2 in such a way that the contribution coming from the lower bound in the inner integral of Eq. (2.17) vanishes, which requires $\eta_2 = -\infty$ (asymptotic past) for $n = 1$ and $\eta_2 = 0$ (asymptotic future) for $n \geq 2$. Since $g_0 = 1$ (given that $\mathcal{G}_0 = C_k$ by definition), this leads to

$$g_n = \frac{(-1)^n (1-2n)}{(2n)!}. \quad (2.21)$$

As a consequence, Eq. (2.14) leads to

$$\mathcal{G}(\eta) = C_k \sum_{n=0}^{\infty} g_n (k\eta)^{2n} = C_k \sum_{n=0}^{\infty} (-1)^n \frac{1-2n}{(2n)!} (k\eta)^{2n} = C_k [\cos(k\eta) + k\eta \sin(k\eta)] \quad (2.22)$$

where we have recognised the Taylor series of $\cos(k\eta) + k\eta \sin(k\eta)$.

For the decaying mode, likewise, the ansatz $\mathcal{D}_n = -D_k H^2 / (6\epsilon_1) d_n \eta^{3+2n}$ satisfies Eq. (2.17) if $d_n = -d_{n-1} / [2n(2n+3)]$, where this time we have set $\eta_2 = 0$ for all n . Together with $d_0 = 1$, this leads to $d_n = 6(-1)^n (n+1) / (2n+3)!$, and Eq. (2.14) yields

$$\mathcal{D}(\eta) = -D_k \frac{H^2}{6\epsilon_1 k^3} \sum_{n=0}^{\infty} d_n (k\eta)^{2n+3} = -D_k \frac{H^2}{2\epsilon_1 k^3} [\sin(k\eta) - k\eta \cos(k\eta)]. \quad (2.23)$$

It is then straightforward to check that Eq. (2.19) can indeed be rewritten as $\mathcal{R}_k = \mathcal{G} + \mathcal{D}$, provided one makes the identification

$$C_k = \frac{iH \text{sign}(\dot{\phi})}{2\sqrt{k^3 \epsilon_1}} (\alpha_k - \beta_k) \quad \text{and} \quad D_k = -\text{sign}(\dot{\phi}) \frac{\sqrt{\epsilon_1 k^3}}{H} (\alpha_k + \beta_k). \quad (2.24)$$

We can thus identify the homogeneous growing and decaying mode solutions (2.15)

$$\mathcal{R}_h = \frac{iH \text{sign}(\dot{\phi})}{2\sqrt{k^3 \epsilon_1}} \left[(\alpha_k - \beta_k) - i (\alpha_k + \beta_k) \frac{(k\eta)^3}{3} \right]. \quad (2.25)$$

In the slow-roll limit, ϵ_1 is a constant², and the first term in the square bracket is the constant growing mode. The second η^3 term is the homogeneous decaying mode. Note however that in slow roll at late times ($\eta \rightarrow 0$) the leading k^2 -correction to the

²We note that (2.25) follows from (2.19) and thus holds more generally for a massless inflaton field in de Sitter, including both the ultra-slow-roll regime where ϵ_1 is small, but time-dependent. However in the ultra-slow-roll limit, where $\sqrt{\epsilon_1} \propto \eta^3$, the identification of the constant and time-dependent terms in (2.25) is swapped [75].

growing mode, *i.e.* the $n = 1$ term in Eq. (2.22), which decays as η^2 , dominates over the homogeneous decaying mode, which decays as η^3 .

The most common approximation for the description of perturbations on super-Hubble scales during inflation is thus to take the homogeneous growing mode for a massless field starting in the Bunch–Davies vacuum state ($\alpha_k = 1$, $\beta_k = 0$) in de Sitter

$$\mathcal{R}_h = \frac{iH \text{sign}(\dot{\phi})}{2\sqrt{k^3 \epsilon_1}}. \quad (2.26)$$

This is equivalent to setting $\delta\phi_h = iH/\sqrt{2k^3}$, leading to the power spectrum for long-wavelength field fluctuations evaluated at Hubble exit, $\mathcal{P}_{\delta\phi_h} = (H/2\pi)^2$.

2.4 Super-Hubble matching

2.4.1 Homogeneous matching

The idea of the separate-universe approach [48] is to approximate the dynamics of perturbations on large scales by the homogeneous solutions, *i.e.* to use only the 0th-order terms in the k^2 -expansion (2.14) above a certain scale. In practice, this can be implemented via a *homogeneous-matching* procedure, where we use the solution to the full equation of motion (2.13) below the matching scale, and match it to its homogeneous counterpart (2.12) above that scale. In what follows, we will express the matching scale in terms of the ratio, σ , of the wavenumber to the Hubble scale, *i.e.* a wavemode k crosses the matching scale when $k = \sigma aH$ and we choose $\sigma < 1$ corresponding to matching on super-Hubble scales.

At the matching scale, we require $\mathcal{R}_h = \mathcal{R}_{k^*}$ and $\mathcal{R}'_h = \mathcal{R}'_{k^*}$, where the subscript “*” refers to quantities evaluated at the matching scale, hence they depend implicitly on k . This leads to the matching conditions

$$\hat{C}_k = \mathcal{R}_{k^*} + z_*^2 \mathcal{R}'_{k^*} \int_{\eta_*}^0 \frac{d\tilde{\eta}}{z^2(\tilde{\eta})} \quad \text{and} \quad \hat{D}_k = -z_*^2 \mathcal{R}'_{k^*}, \quad (2.27)$$

where hats denote quantities estimated by the homogeneous-matching procedure. In the above expressions, \mathcal{R}_{k^*} and \mathcal{R}'_{k^*} are obtained by solving the full linear dynamics, Eq. (2.13), below the matching scale, taking initial conditions in the Bunch–Davies state at past infinity. At late times, \mathcal{R}_k approaches C_k , and thus \hat{C}_k in Eq. (2.27) can be used to approximate the curvature perturbation at the end of inflation.

2.4.2 Matching including k^2 -corrections

In practice, if we match soon after Hubble-crossing, *i.e.*, $\sigma \simeq 1$, the values of \mathcal{R}_{k^*} and \mathcal{R}'_{k^*} , and hence our estimates \hat{C}_k and \hat{D}_k in Eq. (2.27), are liable to be contaminated by gradient terms. One can thus improve our estimate of the solution on large scales by including the leading order k^2 -corrections. While this can be done analytically in the slow-roll limit where ϵ_1 is a constant, in general this would be computationally inefficient, as from Eq. (2.17), a double integration is needed for the k^2 correction to the growing mode and a triple integration would be needed for the decaying-mode correction.

Instead, the freedom in the choice of the upper limit of the integral in Eq. (2.12) can be used to simplify the numerical computation so that the dominant k^2 -correction will be the correction to the adiabatic solution. This suggests we should choose the adiabatic/isocurvature (\mathcal{A}/\mathcal{I}) split at the matching time, $\eta_1 = \eta_*$ in Eq. (2.12). We then have

$$\mathcal{R}_h = \mathcal{A}_0 + \mathcal{I}_0 \int_{\eta}^{\eta_*} \frac{d\tilde{\eta}}{z^2(\tilde{\eta})}, \quad (2.28)$$

and hence we can estimate the leading-order terms in a k^2 -expansion for the adiabatic and isocurvature modes at the matching scale, where

$$\hat{\mathcal{A}}_0 = \mathcal{R}_{k*} \quad \text{and} \quad \hat{\mathcal{I}}_0 = -z_*^2 \mathcal{R}'_{k*}. \quad (2.29)$$

If we further set $\eta_3 = \eta_2 = \eta_*$ in (2.17) to obtain the k^2 -correction to the adiabatic mode,

$$\mathcal{A}_1(\eta) = \mathcal{A}_0 \int_{\eta}^{\eta_*} \frac{d\tilde{\eta}}{z^2(\tilde{\eta})} \int_{\eta_*}^{\tilde{\eta}} d\tilde{\eta} z^2(\tilde{\eta}), \quad (2.30)$$

then this correction makes no contribution to \mathcal{R}_k and \mathcal{R}'_k at the matching time, significantly simplifying the computation.

This choice gives a straightforward form for describing the behaviour of \mathcal{R}_k for $\eta \geq \eta_*$ including the leading-order k^2 -corrections

$$\hat{\mathcal{R}}_k(\eta) = \mathcal{R}_{k*} \left[1 - k^2 \int_{\eta_*}^{\eta} \frac{d\tilde{\eta}}{z^2(\tilde{\eta})} \int_{\eta_*}^{\tilde{\eta}} d\tilde{\eta} z^2(\tilde{\eta}) \right] + z_*^2 \mathcal{R}'_{k*} \int_{\eta_*}^{\eta} \frac{d\tilde{\eta}}{z^2(\tilde{\eta})}. \quad (2.31)$$

It is clear that if one sets $k^2 = 0$, then the homogeneous matching (2.27) is recovered. This result was obtained in Ref. [62], where the super-Hubble enhancement of a mode between the matching time and the end of inflation due to k^2 -corrections was calculated in a model with a transient ultra-slow-roll phase.

2.4.3 The δN formalism

An alternative method to implement the separate-universe approach is the δN formalism [9, 44–47]. This follows from the fact that, on large scales, the curvature perturbation can be identified with the fluctuation in the local expansion $N = \ln(a)$. In particular, the curvature perturbation on uniform-density hypersurfaces [68], ζ , can be identified with the perturbed expansion, δN , between an initial spatially-flat hypersurface during inflation and a final hypersurface of uniform energy density at the end of inflation. In the models that we consider, the perturbations become adiabatic on super-Hubble scales by the end of inflation, and the curvature perturbation on uniform-density hypersurfaces then coincides (up to a sign convention) with the comoving curvature perturbation [47, 48]

$$\zeta = -\mathcal{R} - \frac{3H}{2V} \delta P_{\text{nad}}. \quad (2.32)$$

In practice, as in the homogeneous-matching procedure described in Sec. 2.4, one solves for the full linear dynamics (2.13) below the matching scale, to find \mathcal{R}_{k*} and

\mathcal{R}'_{k^*} , and hence $\delta\phi_{k^*}$ and $\delta\dot{\phi}_{k^*}$ in the spatially-flat gauge (using $\delta\phi = v/a = \dot{\phi}\mathcal{R}/H$ in that gauge). Above the matching scale, the homogeneous dynamics is described by the function $N(\phi_{\text{in}}, \dot{\phi}_{\text{in}})$, which returns the number of e-folds realised using the background equations of motion (2.1) and (2.2) from the initial field values $(\phi_{\text{in}}, \dot{\phi}_{\text{in}})$ up to a late-time hypersurface of uniform energy density (which in practice we take to be the end-of-inflation surface). One then evaluates the fluctuation in the expansion

$$\delta N_k = N(\phi_* + \delta\phi_{k^*}, \dot{\phi}_* + \delta\dot{\phi}_{k^*}) - N(\phi_*, \dot{\phi}_*) \quad (2.33)$$

and at late times, this gives the curvature perturbation $\zeta_k = \delta N_k$.

The above formula can be expanded in the field perturbations $\delta\phi_k$ and $\delta\dot{\phi}_k$, leading to

$$\delta N_k \simeq \frac{\partial N}{\partial\phi_{\text{in}}}(\phi_*, \dot{\phi}_*) \delta\phi_{k^*} + \frac{\partial N}{\partial\dot{\phi}_{\text{in}}}(\phi_*, \dot{\phi}_*) \delta\dot{\phi}_{k^*}. \quad (2.34)$$

At linear order, the δN formalism is strictly equivalent to the homogeneous-matching procedure discussed in Sec. 2.4. In Appendix A, we prove this equivalence for the model discussed in Sec. 3. However, in principle one can use the fully non-linear background equations (2.1) and (2.2), which enables one to use Eq. (2.33) beyond linear order. In practice, we will not consider non-linear effects in what follows, so we will restrict our discussion to the homogeneous-matching procedure, given that it is equivalent to the linearised δN formalism.

3 Piece-wise linear potential

Starobinsky's piece-wise linear model [63] provides an illustrative example of a sudden transition, with the advantage of being fully tractable analytically. It has been extensively studied in the literature, see e.g. Refs. [62, 76–79].

In this toy model, the potential function has the form

$$V(\phi) = \begin{cases} V_0 + A_+(\phi - \phi_{\text{T}}) & \text{for } \phi \geq \phi_{\text{T}}, \\ V_0 + A_-(\phi - \phi_{\text{T}}) & \text{for } \phi < \phi_{\text{T}}, \end{cases} \quad (3.1)$$

with the constants $A_+ > A_- > 0$. Initial conditions are set such that $\phi_{\text{in}} > \phi_{\text{T}}$ and the system reaches the slow-roll attractor in the pre-transition phase of the dynamics. Immediately after the transition, the field velocity inherited from the $\phi > \phi_{\text{T}}$ region is larger than the slow-roll velocity in the $\phi < \phi_{\text{T}}$ region, so there is a transient phase of slow-roll violation, until a second slow-roll attractor is reached at late times. In the limit where $A_+ \gg A_-$, this transient behaviour is an ultra-slow-roll phase.

3.1 Homogeneous background

We will consider the case where $V_0 \gg A_{\pm}|\phi - \phi_{\text{T}}|$, which implies that $\epsilon_1 \ll 1$ throughout and that H is effectively constant. In this de Sitter limit, the Klein–Gordon equation (2.1) can be solved analytically to give

$$\phi(\eta) = \begin{cases} \frac{A_+}{3H^2} \ln(-k_{\text{T}}\eta) + \phi_{\text{T}} & \text{for } \eta \leq \eta_{\text{T}}, \\ \frac{A_-}{3H^2} \ln(-k_{\text{T}}\eta) + \frac{\Delta A}{9H^2} [1 + (k_{\text{T}}\eta)^3] + \phi_{\text{T}} & \text{for } \eta > \eta_{\text{T}}, \end{cases} \quad (3.2)$$

where $\Delta A = A_- - A_+ < 0$ and η_T is the comoving transition time. Here we have introduced the comoving scale $k_T = -1/\eta_T$ that crosses the Hubble radius at the transition time. We have assumed that inflation starts sufficiently far from ϕ_T such that the slow-roll attractor has been reached well before the transition, and we have used the continuity of ϕ and $\dot{\phi}$ at the transition to set the integration constants for $\phi < \phi_T$ (corresponding to $\eta > \eta_T$).

The first and second Hubble-flow parameters (2.3) are then

$$\epsilon_1(\eta) = \begin{cases} \frac{A_+^2}{18H^4} & \text{for } \eta \leq \eta_T, \\ \frac{(\Delta A k_T^3 \eta^3 + A_-)^2}{18H^4} & \text{for } \eta > \eta_T, \end{cases} \quad (3.3)$$

and

$$\epsilon_2(\eta) = \begin{cases} 0 & \text{for } \eta \leq \eta_T, \\ -\frac{6\Delta A k_T^3 \eta^3}{\Delta A k_T^3 \eta^3 + A_-} & \text{for } \eta > \eta_T. \end{cases} \quad (3.4)$$

While ϵ_1 is continuous, ϵ_2 is discontinuous at the transition, due the discontinuity in $dV/d\phi$. In what follows, the pre- and post-transition behaviours will be labelled by the subscripts “+” and “−”, respectively.

3.2 Perturbations

To find solutions of the mode equation (2.4) we first need to find the behaviour of $z = a\dot{\phi}/H$. From Eq. (3.3) we have

$$z(\eta) = \begin{cases} \frac{A_+}{3H^3} \eta^{-1} & \text{for } \eta \leq \eta_T, \\ \frac{A_- + \Delta A k_T^3 \eta^3}{3H^3} \eta^{-1} & \text{for } \eta > \eta_T. \end{cases} \quad (3.5)$$

One can check that z is continuous at $\eta = \eta_T$ but that its derivative is discontinuous.

The effective mass-squared $\mu^2 = -z''/z$ appearing in the Sasaki–Mukhanov equation (2.4) can also be obtained from Eq. (2.5). Neglecting the sub-dominant contributions from $\epsilon_1 \ll 1$, one finds

$$\mu^2 = \frac{1}{\eta^2} \left[-2 + \frac{3\Delta A \eta_T}{A_+} \delta_D(\eta - \eta_T) \right], \quad (3.6)$$

where δ_D is the Dirac δ distribution. Apart from at the transition, $\mu^2 = -2/\eta^2$, but it experiences a sudden impulse at $\eta = \eta_T$ due to the discontinuity in the second slow-roll parameter, ϵ_2 . Therefore the general solution for \mathcal{R}_k is given by Eq. (2.19) both before and after the transition, but with different constants of integration.

Pre-transition

Before the transition we set initial conditions in the Bunch–Davies vacuum (2.6) at early times, corresponding to $\alpha_{k+} = 1$ and $\beta_{k+} = 0$ in Eq. (2.19), leading to

$$\mathcal{R}_k = -\frac{iH}{2\sqrt{k^3 \epsilon_{1+}}} (1 + ik\eta) e^{-ik\eta}. \quad (3.7)$$

In the absence of a transition (i.e. if $\Delta A = 0$), the amplitude of the growing and decaying modes (2.15) can be identified from Eq. (2.24). One finds

$$\tilde{C}_k = -\frac{3iH^3}{A_+\sqrt{2k^3}} \quad \text{and} \quad \tilde{D}_k = \frac{A_+}{3H^3\sqrt{2k^3}}k^3. \quad (3.8)$$

Here, tildes are used to denote the *apparent* growing and decaying modes in the pre-transition phase.

Post-transition

After the transition, the behaviour of the perturbations is still given by the general solution, Eq. (2.19), but with different values for the Bogoliubov coefficients compared to the pre-transition phase.

Both \mathcal{R}_k and \mathcal{R}'_k are continuous at the transition, since z'/z remains finite in Eq. (2.13). However, although the Sasaki–Mukhanov variable, $v_k = \mathcal{R}_k/z$ is continuous at the transition, its time derivative v'_k is discontinuous due to the Dirac δ -function in the effective mass-squared, μ^2 in Eq. (3.6), which appears in the mode equation Eq. (2.4). The jump in v'_k is given by

$$\begin{aligned} v'_{k-}(\eta_T + h) - v'_{k+}(\eta_T - h) &= \int_{\eta_T-h}^{\eta_T+h} d\eta v''_k(\eta) \\ &= \int_{\eta_T-h}^{\eta_T+h} d\eta \left[\frac{2}{\eta^2} - \frac{3\Delta A}{A_+\eta_T} \delta_D(\eta - \eta_T) - k^2 \right] v_k(\eta) \\ &\xrightarrow{h \rightarrow 0} -\frac{3\Delta A}{A_+\eta_T} v_k(\eta_T). \end{aligned} \quad (3.9)$$

This leads to the new Bogoliubov coefficients after the transition [63, 77]

$$\alpha_{k-} = 1 + \frac{3i}{2} \frac{\Delta A k_T}{A_+ k} \left(1 + \frac{k_T^2}{k^2} \right), \quad (3.10)$$

$$\beta_{k-} = -\frac{3i}{2} \frac{\Delta A k_T}{A_+ k} \left(1 + i \frac{k_T}{k} \right)^2 e^{2ik/k_T}. \quad (3.11)$$

We see that the sudden transition is non-adiabatic ($\beta_{k-} \neq 0$), leading to particle production on sub-Hubble scales and time-dependence of the curvature perturbation, even on super-Hubble scales.

The homogeneous growing and decaying modes can be obtained by rewriting the homogeneous part of the general solution, Eq. (2.19), in the form (2.12), which gives

$$\begin{aligned} C_k &= -\frac{3iH^3}{A_-\sqrt{2k^3}} (\alpha_{k-} - \beta_{k-}), \\ D_k &= \frac{A_- k^3}{3H^3\sqrt{2k^3}} \left[\alpha_{k-} + \beta_{k-} - 3i \frac{\Delta A}{A_-} \left(\frac{k_T}{k} \right)^3 (\alpha_{k-} - \beta_{k-}) \right]. \end{aligned} \quad (3.12)$$

In the absence of a transition, $\Delta A = 0$, one recovers $\beta_{k-} = 0$ and the apparent pre-transition growing and decaying modes given in Eq. (3.8). To better understand the effect of the transition, it is helpful to expand Eq. (3.12), using Eq. (3.10) and Eq. (3.11), in various limits.

Scales $k \ll k_T$

When $k \ll k_T$, *i.e.* for scales that exit the Hubble radius long before the transition, by Taylor expanding Eq. (3.12), one finds

$$\begin{aligned} C_k &= -\frac{3iH^3}{\sqrt{2k^3}A_+} \left\{ 1 + \frac{2}{5} \frac{\Delta A}{A_-} \left(\frac{k}{k_T} \right)^2 \left[1 + \frac{5i}{6} \frac{k}{k_T} + \mathcal{O} \left(\frac{k^2}{k_T^2} \right) \right] \right\}, \\ D_k &= \frac{A_- k^3}{3H^3 \sqrt{2k^3}} \left[3i \frac{\Delta A}{A_-} \left(1 + \frac{3}{5} \frac{\Delta A}{A_+} \right) \frac{k_T}{k} + \frac{A_+}{A_-} + \mathcal{O} \left(\frac{k}{k_T} \right) \right]. \end{aligned} \quad (3.13)$$

Note that the term $\Delta A/A_-$ may be large (this is the case if $A_- \ll A_+$), which leads us to distinguish three sub-cases.

If $k/k_T \ll \sqrt{A_-/|\Delta A|}$, then the non-adiabatic, decaying mode D_k is suppressed in Eq. (3.13) and C_k reduces to the apparent growing mode in the pre-transition phase, Eq. (3.8). These scales are sufficiently far outside the Hubble scale at the time of the transition that they are not affected by the sudden jump and \mathcal{R}_k remains constant after the transition. This corresponds to the left-hand scale-invariant plateau shown in the left-hand panel of Fig. 3.

For $\sqrt{A_-/|\Delta A|} \sim k/k_T$, the two leading terms in Eq. (3.13) for C_k are of the same order and can cancel, since $\Delta A/A_- < 0$. The higher-order terms are strongly suppressed for $k/k_T \ll 1$. This explains the well-known dip in the power spectrum (2.18), as shown in Fig. 3.

If $\sqrt{A_-/|\Delta A|} \ll k/k_T$, then the term proportional to $(k/k_T)^2$ dominates in Eq. (3.13), which leads to the intermediate region in Fig. 3 where the power spectrum scales as $\mathcal{P}_{\mathcal{R}} \propto k^4$ [30, 80]. These scales are super-Hubble at the time of the transition, but they have spent too little time outside the Hubble radius to suppress gradient terms to the level that would be necessary to make the non-adiabatic term irrelevant after the transition. Therefore, as first observed in Ref. [62], the presence of gradient terms at the sudden transition can leave a strong imprint on super-Hubble scales. More precisely, the scale above which \mathcal{R} is approximately constant is not the Hubble radius but is somewhat larger, given by $\sqrt{|\Delta A|/A_-}$ times the Hubble radius³.

Since this behaviour is key to understanding the main result of this paper, let us further comment on it. As already explained, \mathcal{R} and \mathcal{R}' are continuous at the transition. Let us check whether or not this is the case for their homogeneous counterparts, *i.e.* let us compare the apparent homogeneous solution before the transition (3.8) to the

³The reason why the ratio $\Delta A/A_-$ appears can be understood from Eq. (3.3), which can be rewritten as $\epsilon_{1-} = A_-^2/(18H^4)[1 - \Delta A/A_- e^{-3(N-N_T)}]^2$. This shows that the ultra-slow-roll phase after the transition lasts for of order $\ln(\Delta A/A_-)/3$ e-folds before it returns to slow roll.

homogeneous solution after the transition (3.13)

$$\begin{aligned}\frac{\Delta\mathcal{R}_h}{\tilde{\mathcal{R}}_h(\eta_T)} &\equiv \frac{\mathcal{R}_h(\eta_T) - \tilde{\mathcal{R}}_h(\eta_T)}{\tilde{\mathcal{R}}_h(\eta_T)} \simeq -\frac{3}{5} \frac{\Delta A}{A_+} \left(\frac{k}{k_T}\right)^2, \\ \frac{\Delta\mathcal{R}'_h}{\tilde{\mathcal{R}}'_h(\eta_T)} &\equiv \frac{\mathcal{R}'_h(\eta_T) - \tilde{\mathcal{R}}'_h(\eta_T)}{\tilde{\mathcal{R}}'_h(\eta_T)} \simeq 3i \frac{\Delta A}{A_+} \left(1 + \frac{3}{5} \frac{\Delta A}{A_+}\right) \frac{k_T}{k}.\end{aligned}\tag{3.14}$$

Since $|\Delta A/A_+| < 1$, the relative jump in \mathcal{R}_h at the transition is suppressed by $(k/k_T)^2$, which is indeed small for scales that are super-Hubble at the time the transition. However the relative jump in \mathcal{R}'_h is enhanced by k_T/k , even if the absolute jump is suppressed by k/k_T .

This explains what is observed in Fig. 2, where the apparent homogeneous solution found before the transition, $\tilde{\mathcal{R}}_h$, remains constant post-transition, while the actual homogeneous solution after the transition, \mathcal{R}_h , shows rapid time evolution. Also note that the actual homogeneous solution after the transition, \mathcal{R}_h , propagated back to Hubble-exit shows an order of magnitude difference compared to the apparent pre-transition homogeneous solution, $\tilde{\mathcal{R}}_h$, at that time. But if we track the change to the homogeneous behaviour, $\Delta\mathcal{R}_h$ and $\Delta\mathcal{R}'_h$ induced at the transition, and propagate that forward using the homogeneous equation of motion, the correct post-transition behaviour on super-Hubble scales is recovered. This suggests we can keep track of the homogeneous behaviour, even if there is a sudden transition, by including the correct non-adiabatic jump coming from gradient terms at the transition.

Scales $k \gg k_T$

Finally we note that for $k \gg k_T$, *i.e.* scales that exit the Hubble radius some time after the transition, one has

$$C_k = -\frac{3iH^3}{\sqrt{2k^3A_-}} \left[1 + \frac{3i}{2} \frac{\Delta A}{A_+} \frac{k_T}{k} \left(1 + e^{2i\frac{k}{k_T}} \right) + \mathcal{O}\left(\frac{k_T^2}{k^2}\right) \right].\tag{3.15}$$

Here, $|\Delta A/A_+|$ is always smaller than one, hence the first term in the square bracket dominates and one recovers the slow-roll result in the post-transition region (*i.e.* Eq. (3.15) reduces to Eq. (3.8) where A_+ is replaced with A_-). This corresponds to the right-hand scale-invariant plateau in the left panel of Fig. 3, with damped sinusoidal modulation of the power spectrum for $k \gtrsim k_T$.

3.3 Homogeneous matching

Let us now employ the homogeneous-matching procedure described in Sec. 2.4 to estimate the homogeneous perturbations in the Starobinsky piece-wise linear model. Using Eq. (3.5) to evaluate the terms involving $z(\eta)$, Eq. (2.27) gives rise to

$$\hat{C}_k = \begin{cases} \mathcal{R}_{k^*} + \left[1 - \frac{\Delta A}{A_-} \left(\frac{k}{\sigma k_T}\right)^3 \right] \frac{\sigma}{3k} \mathcal{R}'_{k^*} & \text{for } k \leq \sigma k_T \\ \mathcal{R}_{k^*} + \left[1 - \frac{\Delta A}{A_-} \left(\frac{k}{\sigma k_T}\right)^{-3} \right] \frac{\sigma}{3k} \mathcal{R}'_{k^*} & \text{for } k > \sigma k_T \end{cases},\tag{3.16}$$

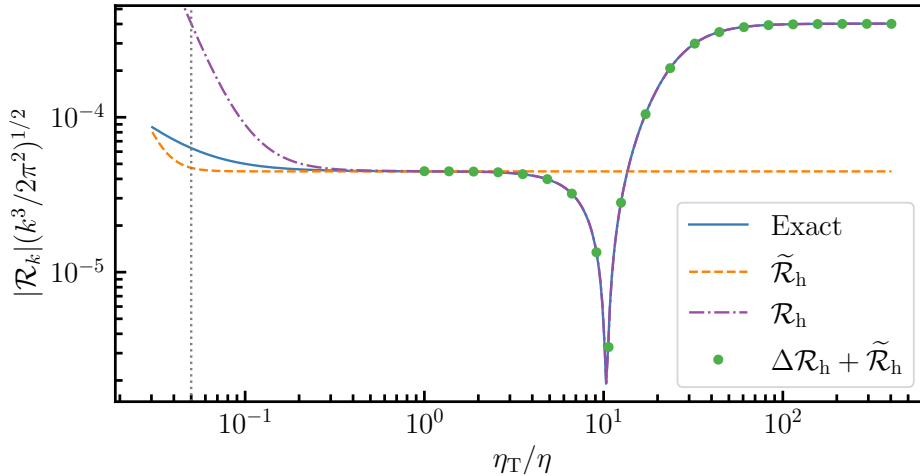


Figure 2. The evolution of the curvature perturbation \mathcal{R}_k with comoving time η for a wavemode with $k = 0.05 k_T$ in the piece-wise linear potential (3.1) with $A_-/A_+ = 10^{-4}$. The sudden transition from slow roll to ultra-slow roll occurs at $\eta_T = -1/k_T$. The solid blue curve is found by numerically solving the full Sasaki–Mukhanov equation (2.4). The dashed orange curve corresponds to the homogeneous solution (2.12) with the apparent growing and decaying mode amplitudes before the transition, Eq. (3.8), and the dot-dashed purple curve corresponds to the homogeneous solution (2.12) with the growing and decaying mode amplitudes after the transition Eq. (3.12). The green data points are found by adding the discontinuous jump at the transition (3.14) to the homogeneous solution (2.12) with the apparent growing and decaying mode amplitudes before the transition, Eq. (3.8). The dotted vertical line shows the Hubble-exit time, when $aH = 0.05 k_T$.

where we recall that \mathcal{R}_{k^*} and \mathcal{R}'_{k^*} correspond to the curvature perturbation and its time derivative at the time where k crosses the matching scale (*i.e.* when $k = \sigma aH$), as given by the full perturbation theory established in Sec. 3.2. In Fig. 3, we show the power spectrum of \mathcal{R} and the evolution of a single mode with $k = 0.05 k_T$ calculated using the homogeneous matching procedure for different values of σ .

At this stage, it is worth highlighting the calculation performed in Appendix A, where the δN program described in Sec. 2.4.3 has been implemented for Starobinsky’s piece-wise linear model. In the linear version of the calculation, one obtains Eq. (A.23), which exactly coincides with Eq. (3.16). This illustrates the statement made above that, for linear perturbations, the homogeneous-matching procedure and the δN approach are equivalent.

Matching before the transition

For $k \leq \sigma k_T$, the matching scale is crossed before the transition, and inserting Eq. (3.7) into the first entry of Eq. (3.16) leads to

$$\hat{C}_k = -\frac{3iH^3 e^{i\sigma}}{\sqrt{2k^3} A_+} \left[1 - i\sigma - \frac{\sigma^2}{3} + \frac{\sigma^2}{3} \frac{\Delta A}{A_-} \left(\frac{k}{\sigma k_T} \right)^3 \right]. \quad (3.17)$$

This has to be compared with the full homogeneous solution after the transition given by Eq. (3.12), which reduces to Eq. (3.13) in the limit where $k \ll k_T$. If matching is done in the super-Hubble regime, $\sigma \ll 1$, one observes different behaviours depending on how k/k_T compares with $\sqrt{A_-}/|\Delta A|$.

If $k/k_T \ll \sqrt{A_-}/|\Delta A|$, the late-time curvature perturbation obtained from homogeneous matching, Eq. (3.17), reduces to the full result (3.13), up to $\mathcal{O}(\sigma^2)$ corrections. The usual separate-universe approach is therefore able to reproduce the left-hand scale-invariant plateau in Fig. 3, since the curvature perturbation remains a constant on super-Hubble scales even during the ultra-slow-roll phase.

If $\sqrt{A_-}/|\Delta A| \ll k/k_T \ll 1$, the k^2 term becomes dominant in Eq. (3.13), and cannot be reproduced by the terms in Eq. (3.17). The usual separate-universe approach thus fails in this case. The reason is that, in the exact result, Eq. (3.13), the k^2 term comes from gradient corrections to the growing mode, see Sec. 2.3.1. However, this contribution is not accounted for in the homogeneous matching, Eqs. (3.16) and (3.17), since it does not appear in the homogeneous solution (2.12). Homogeneous matching only captures the leading order of the decaying mode, which scales as k^3 . This is demonstrated in Fig. 3 for both the power spectrum and the time evolution of a particular mode.

Matching after the transition

For $k > \sigma k_T$, the matching scale is crossed after the transition and one may use Eq. (2.19), together with Eq. (3.3) for $\epsilon_1(\eta)$ for $\eta \geq \eta_T$, to evaluate \mathcal{R}_{k*} and \mathcal{R}'_{k*} in the second entry of Eq. (3.16). This leads to

$$\hat{C}_k = -\frac{3iH^3}{A_- \sqrt{2k^3}} \left[\alpha_{k-} e^{i\sigma} \left(1 - i\sigma - \frac{\sigma^2}{3} \right) - \beta_{k-} e^{-i\sigma} \left(1 + i\sigma - \frac{\sigma^2}{3} \right) \right], \quad (3.18)$$

where α_{k-} and β_{k-} after the transition are given in Eqs. (3.10) and (3.11). At leading order in σ , this reduces to $\hat{C}_k \simeq -3iH^3(\alpha_{k-} - \beta_{k-})/(A_- \sqrt{2k^3})$, which coincides with the exact expression, Eq. (2.24). As a consequence, up to $\mathcal{O}(\sigma^2)$ corrections, the homogeneous-matching procedure is able to correctly reproduce the late-time behaviour of the curvature perturbation if the matching is performed after the transition, as shown in Fig. 3.

Let us summarise our findings. The above results show that the homogeneous-matching procedure fails for the scales within the range $\sqrt{A_-}/|\Delta A| < k/k_T < 1$ if they are matched before the transition, and succeeds otherwise as long as $\sigma \ll 1$. Therefore,

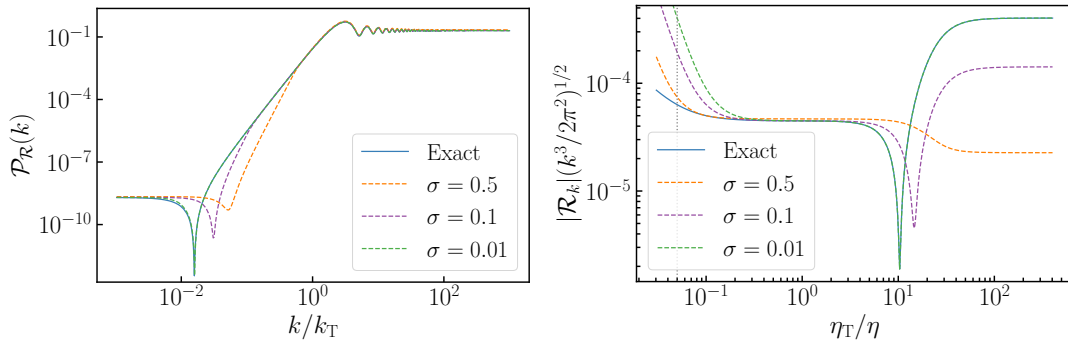


Figure 3. Left: the power spectrum (2.18) of the curvature perturbation, \mathcal{R} , against wavenumber, k/k_T for the piece-wise linear potential (3.1) with $A_-/A_+ = 10^{-4}$. Right: the evolution of \mathcal{R}_k for a mode with $k = 0.05 k_T$, along with the homogeneous solution resulting from matching at different values of $\sigma = k/aH$. In both panels, the solid blue curve is found by numerically solving the full mode equation Eq. (2.4) and the dashed curves are obtained numerically using the matching procedure detailed in Sec. 2.4. The dotted vertical line is Hubble-exit time. The ultra-slow-roll period starts at $\eta_T = -1/k_T$.

in order to match the dangerous set of scales after the transition, one requires

$$\sigma \ll \min \left(1, \sqrt{\frac{A_-}{|\Delta A|}} \right). \quad (3.19)$$

As mentioned in Footnote 3, $A_-/\Delta A$ can be related to the number of e-folds during the ultra-slow-roll phase, N_{USR} , so we expect the above condition to generalise to

$$\sigma \ll e^{-\frac{3}{2}N_{\text{USR}}}, \quad (3.20)$$

in more general models. This condition is more stringent than the one usually encountered in the absence of sudden transitions, $\sigma \ll 1$, but it ensures the validity of the separate-universe approach after homogeneous matching.

3.4 Including k^2 -corrections

As discussed below Eq. (2.24), the k^2 -correction to the growing mode can dominate over the leading-order decaying mode at late times. As a consequence, the late-time non-adiabatic behaviour may be dominated by contributions coming from k^2 -corrections in the gradient expansion, hence the separate-universe approach fails on some super-Hubble scales in the presence of a sudden transition. One can further check the validity of this statement by including the leading k^2 -corrections in the matching procedure, as was discussed in Sec. 2.4.2. This has been shown in Fig. 4 matching very close to Hubble-exit, $\sigma = 0.5$. This gives an excellent approximation to the exact power spectrum, confirming the k^2 -corrections are indeed needed to fully explain the super-Hubble evolution in the presence of a sudden transition after the matching.

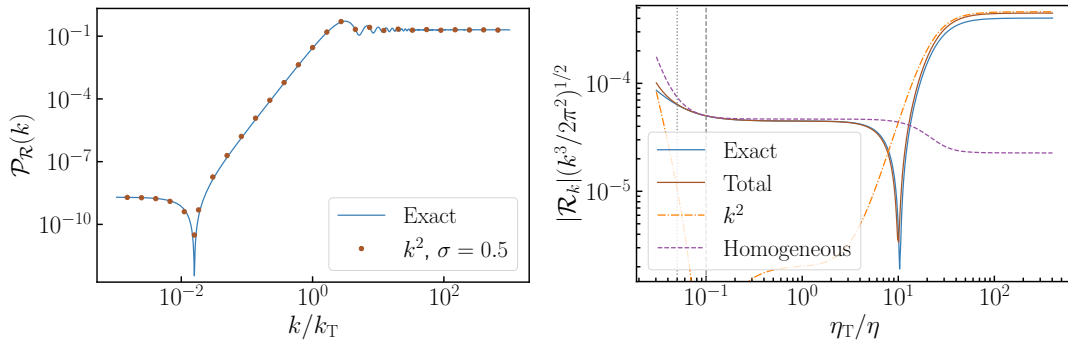


Figure 4. Left: the power spectrum (2.18) of the curvature perturbation \mathcal{R} for the piece-wise linear potential (3.1) with $A_-/A_+ = 10^{-4}$. The solid blue curve is found by numerically solving Eq. (2.4) and the brown points are found by including the k^2 term in the adiabatic mode at matching, as detailed in Sec. 2.4.2. Right: evolution of the components of Eq. (2.31) plotted along with the full solution of the mode equation for $k = 0.05 k_T$. The k^2 curve is the k^2 -term, “Homogeneous” is the k^2 -independent component, and “Total” is the sum of the two. The dotted and dashed vertical lines correspond to Hubble-exit and matching times, respectively. The ultra-slow-roll period starts at $\eta_T = -1/k_T$.

By comparing the k^2 -corrected reconstruction shown in Fig. 4 with the homogeneous matching used in Fig. 3, it is clear that the post-transition behaviour is recovered well (within $\sim 10\%$) even for $\sigma = 0.5$, when the k^2 -corrections are included. This is in contrast to the homogeneous matching case, where a σ -value corresponding to matching after the transition ($\sigma < 0.05$) is required. This clearly shows that the k^2 -corrections at the transition are required to describe the non-adiabatic homogeneous behaviour on super-Hubble scales after the transition. If $\sigma = 0.1$ is used for the k^2 -corrected Eq. (2.31), the late-time behaviour is reconstructed within $\sim 1\%$.

4 Smooth potential with a Gaussian bump

Let us consider a model with a smooth slow-roll to ultra-slow-roll transition. One way this can be achieved is by the addition of a Gaussian bump to a working slow-roll potential, giving a model which is both in agreement with CMB observations and can produce a significant abundance of PBHs [81]. One such potential is given by

$$V(\phi) = V_0 \frac{\phi^2}{m^2 + \phi^2} \left\{ 1 + K \exp \left[-\frac{1}{2} \frac{(\phi - \phi_0)^2}{\Sigma^2} \right] \right\}, \quad (4.1)$$

with $m = 0.5 M_{\text{Pl}}$, $K = 1.876 \times 10^{-3}$, $\phi_0 = 2.005 M_{\text{Pl}}$ and $\Sigma = 1.993 \times 10^{-2} M_{\text{Pl}}$ [81]. Note that all of the above precision is needed to produce an asteroid-mass PBH abundance accounting for all of the dark matter, due to fine-tuning [82]. This model has a period of ultra-slow roll of ~ 3 e-folds, before smoothly transitioning to a phase of constant roll. The transition from slow roll to ultra-slow roll takes ~ 1 e-fold. As such, one cannot

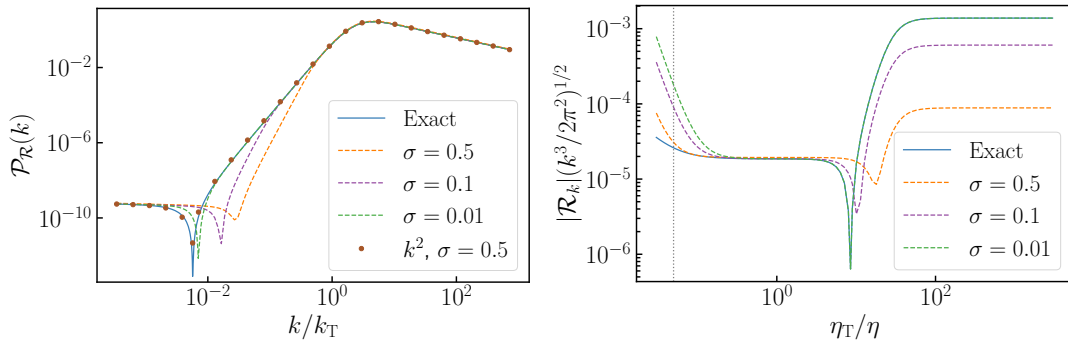


Figure 5. Left: the power spectrum (2.18) of the curvature perturbation \mathcal{R} for a potential with a Gaussian bump (4.1). Right: the evolution of \mathcal{R} for a mode with $k = 0.05 k_T$. The solid blue curve is found by numerically solving Eq. (2.4), the dashed curves are found using the numerical matching procedure detailed in Sec. 2.4, and the brown data points are found by including the k^2 correction (2.31). The dotted vertical line is Hubble-exit time. The ultra-slow-roll period ($\epsilon_2 < -3$) starts at $\eta_T = -1/k_T$.

easily propagate modes through the transition analytically, and a numerical approach is required.

Determining the homogeneous growing and decaying modes can be done numerically using the homogeneous-matching procedure, detailed in Eq. (2.27). This is shown in Fig. 5. Phenomenologically we see similar behaviour to the previously discussed piecewise linear model. The power spectrum is most accurately reconstructed when matching sufficiently long after Hubble-exit, $\sigma = 0.01$, although it is still not able to fully reproduce the dip behaviour. This is because $\sigma = 0.01$ is not sufficient to satisfy the condition given in Eq. (3.20) for this model, as it has a longer duration of ultra-slow-roll inflation compared to the piece-wise linear potential shown above. The k^2 -corrected data points, found using Eq. (2.31) to do the matching, are accurate even when matching soon after Hubble-exit for $\sigma = 0.5$. This shows the effect of gradient terms on the homogeneous behaviour on super-Hubble scales at the sudden transition from slow roll to ultra-slow roll, in smooth models, not just in the idealised, instant transition case.

The interpretation of the evolution of the mode seen in the right-hand panel in Fig. 5 is the same as for the piece-wise linear model if we define the transition to ultra-slow roll to happen when $\epsilon_2 < -3$ first occurs. If the homogeneous matching is done before the transition time, the early-time behaviour is recovered but the behaviour after the transition is not. Equally, matching after the transition reproduces the late-time behaviour (more accurately for smaller σ) but does not reproduce the early-time behaviour. This shows numerically that the sudden transition to ultra-slow roll has resulted in the behaviour of the homogeneous growing/decaying modes changing due to gradient terms at the transition.

In Appendix B we show another example of a model with a smooth potential that leads to a sudden transition from slow roll to ultra-slow roll. In that case we see that a

potential with an inflection point shows the same qualitative behaviour for modes before and after a sudden transition from slow roll to ultra-slow roll, suggesting that this is a common feature of such models.

5 Implications for stochastic inflation

In the stochastic approach to studying inflationary dynamics [83, 84] quantum field perturbations originating on small, sub-Hubble scales are incorporated into the locally-homogeneous background classical field in a local patch after crossing the coarse-graining scale, giving the local background field a stochastic kick. In effect the coarse-graining introduces a matching scale, $k = \sigma aH$, between the solution to the full mode equation on small scales and a homogeneous solution used on larger scales. In the standard case the stochastic kick is included soon after Hubble exit, corresponding to $\sigma \sim 1$. But we have shown that a sudden transition leads to a change in the state of the field on a finite range of super-Hubble scales. If there is a discontinuity in the homogeneous field perturbation after coarse-graining, then the standard stochastic approach breaks down.

One approach to address this issue is to coarse-grain only after the transition or on sufficiently large super-Hubble scales such that any discontinuity in the homogeneous solution at the transition is minimal. If the condition given in Eq. (3.20) is used, then the correct post-transition solution for $\delta\phi_h$ is captured for all modes. For example in Refs. [78, 85–88] $\sigma = 0.01$ is chosen, in which case coarse-graining captures the transition-induced change to $\delta\phi_h$ for modes with $k \gtrsim 0.01 k_T$, which is sufficient to avoid any significant discontinuity for a sudden transition leading to an ultra-slow-roll period of $\lesssim 3$ e-folds.

However, incorporating the stochastic kick into the long-wavelength evolution a long time after Hubble exit fails to account for nonlinear effects due to field fluctuations close to the Hubble scale, so is likely to under-estimate the full stochastic effects. This may be particularly important when modelling the transition to ultra-slow roll as this is a transient regime. For example, this could reduce the probability of large, rare fluctuations in δN which may be associated with PBH production. We could attempt to evolve the post-transition homogeneous solution back to the Hubble-exit time, and apply the corresponding stochastic kick at that time in order to include the non-adiabatic behaviour induced after the transition. However, this gives an erroneously large non-adiabatic kick before the transition, at a time when the super-Hubble evolution was in fact adiabatic. This can be seen by comparing $\tilde{\mathcal{R}}_h$ and \mathcal{R}_h in Fig. 2 near Hubble exit. The enhanced non-adiabatic decaying mode of \mathcal{R}_h is induced by the transition and was not present when the mode crossed the Hubble scale.

A possible solution is to apply *two* kicks for each mode with $k < k_T$: the first applied in the usual stochastic way at or soon after Hubble exit before the transition, and the second, correlated kick applied at or just after the transition to reproduce the correct non-adiabatic behaviour post-transition. As we already saw in Fig. 2, for linear perturbations, the correct behaviour before and after the transition can be recovered if we include the discontinuity in the homogeneous solution at the transition. The pre-transition kick can be found in a number of ways. The simplest is to use the slow-roll

result, $\delta\phi_h \simeq iH/\sqrt{2k^3}$ at Hubble exit. Alternatively, this can be done numerically, either directly matching $\delta\phi_h$ to $\delta\phi_k$, or using a Bessel function approximation at Hubble exit as described in Appendix C. The latter allows $\delta\phi_h$ to be found close to Hubble-scale crossing and it explicitly removes spurious gradient terms from the homogeneous solutions. The post-transition non-adiabatic kick would need to be found from the solution to the full mode equations at the transition. This could again either be done directly from a numerical solution, or with the Bessel function approximation. Since the discontinuity in $\delta\phi_h$ occurs at the transition for super-Hubble modes, $k < k_T$, the second kicks for all these modes would be applied at the same time. Thus a single non-adiabatic kick at the transition, found by summing the contributions from all of the $k < k_T$ modes, could incorporate the non-adiabatic change to the homogeneous behaviour induced by the transition.

Finally we note that in the stochastic-inflation formalism it is assumed that the quantum field fluctuations can be described by a classical noise. This is consistent with the initial adiabatic vacuum state becoming a highly squeezed state on super-Hubble scales [89–91]. However, the discontinuity in the homogeneous solution at the transition may have implications for the quantum-to-classical transition [74, 92–94]. A full study of classicalisation at such transitions is beyond the scope of this paper, and we leave further investigation of this interesting question for future work.

6 Conclusion

Models of inflation incorporating a transition from slow roll to ultra-slow roll have been intensively studied recently as a mechanism to produce primordial black holes (PBHs). As well as using linear perturbation theory to study the power spectrum produced in such models, non-perturbative approaches, such as the δN or stochastic δN formalisms, have been used to determine the full probability distribution function for the curvature perturbation. These typically rely on the separate-universe approach, using solutions to the spatially-homogeneous equations of motion to model the evolution of inhomogeneities beyond the Hubble scale.

In this paper we have shown that the separate-universe approach breaks down on a finite range of super-Hubble scales at a sudden transition during inflation from slow roll to ultra-slow roll. The sudden transition leads to particle production in the inflaton field on sub-Hubble scales and non-adiabatic pressure perturbations on super-Hubble scales.

We emphasise that the separate-universe approach works in a piece-wise fashion, before the transition and in the ultra-slow-roll phase after⁴, but a solution to the spatially-homogeneous equations is unable to reproduce the discontinuous change in the super-Hubble behaviour at the transition, which is due to small, but finite spatial gradients still present on super-Hubble scales. The role of spatial gradients even on super-Hubble scales in a model of ultra-slow-roll inflation was first noted in Ref. [62].

⁴It was previously shown in Ref. [74] that the separate universe approach applies beyond slow roll, in contrast to the conclusions of Ref. [95]. In general one must allow for perturbations in the lapse function on large scales, which vanish only in the slow-roll limit where $\epsilon_1 \rightarrow 0$.

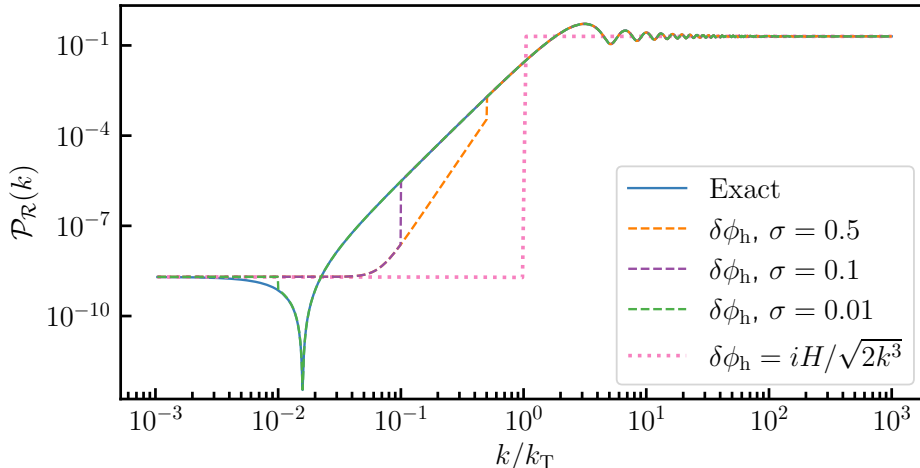


Figure 6. The power spectrum (2.18) of the curvature perturbation \mathcal{R} for the piece-wise linear potential (3.1) with $A_-/A_+ = 10^{-4}$. The solid blue curve is found by numerically solving the full mode equation (2.4). The dashed curves use the linear δN formalism (2.34) with $\delta\phi_h = \dot{\phi}\mathcal{R}_h/H$ given in a piece-wise manner, where Eq. (3.8) is used before the transition and Eq. (3.12) after. The δN formalism is applied at $k = \sigma aH$. The pink dotted curve uses the result (2.26) for a massless field at Hubble-exit in de Sitter, $\delta\phi_h = iH/\sqrt{2k^3}$ with $\sigma = 1$. The ultra-slow-roll period starts at comoving time $\eta_T = -1/k_T$.

The discontinuity in the homogeneous behaviour was shown analytically in (3.14) for an idealised test case corresponding to the piece-wise linear potential (3.1). In this case the general solution to the full mode equation before and after the transition is given in (2.19) allowing us to identify the homogeneous solution (2.25) from a formal gradient expansion (2.14). We have also demonstrated numerically that a discontinuity in the homogeneous solution occurs at a sudden transition in models with a smooth feature in the potential (either a Gaussian bump, or an inflection point, shown in Figs. 5 and 8 respectively) using numerical matching to estimate the homogeneous solution after Hubble exit.

This discontinuous behaviour at the transition time, $\eta_T = -1/k_T$, has implications for the δN formalism, where one uses the homogeneous solution to follow the evolution of the perturbed universe on super-Hubble scales. The naïve approach, using the Bunch–Davies vacuum state for a massless field in de Sitter at Hubble-exit to set the amplitude of fluctuations in the spatially-homogeneous field, $\mathcal{P}_{\delta\phi_h}^{1/2} = H/2\pi$, fails completely to describe the growth of the power spectrum for $k < k_T$ or accurately give the peak value at $k \sim k_T$. See Fig. 6, where the error in the power spectrum peak is $\sim 60\%$ if $\mathcal{P}_{\delta\phi_h}^{1/2} = H/2\pi$ is used, but less than 0.1% for the correct post-transition homogeneous $\delta\phi_h$. This shows the importance of non-adiabatic evolution even on sub-horizon scales at the transition.

We can only reconstruct the full behaviour by matching fluctuations in the ho-

mogeneous field to the mode functions at (or soon after) Hubble-exit if k^2 -corrections (2.31) are included at the matching, showing the essential role of spatial gradients on super-Hubble scales at the transition. If the corrected homogeneous solution is used post-transition in the classical δN formalism (2.33), including a non-adiabatic decaying mode (*i.e.* including both $\delta\phi_{k*}$ and $\delta\dot{\phi}_{k*}$), the correct linear power spectrum can be recovered at the end of inflation. This suggests that a modified separate-universe approach might still be used, and non-linear perturbations could be found using the classical δN formalism in the presence of a sudden transition, if applied in a piece-wise manner. We leave investigation of higher-order effects in the classical δN formalism to future work.

In the stochastic-inflation formalism, applying the separate universe approach in a piece-wise manner would correspond to coarse-graining only on scales very much larger than the Hubble radius, such that all the affected modes are coarse-grained after the transition. However this may underestimate stochastic effects by failing to include all super-Hubble fluctuations in the coarse-grained field before the transition. An alternative method would be to coarse-grain close to the Hubble scale before the transition, but then to include the discontinuity in the homogeneous behaviour by summing all the affected modes into a single non-adiabatic kick to the coarse-grained field at the transition. We leave the implementation of a modified stochastic-inflation approach in such models for future work.

Note Added

While this work was in preparation Ref. [96] appeared, where it was shown that the usual δN formalism could only be applied sufficiently long after a sudden transition, such that $\delta\phi_h$ is dominated by the growing mode, which is consistent with our results.

Acknowledgments

The authors would like to thank Laura Iacconi, Eemeli Tomberg, Diego Cruces, David Mulryne and the participants of Cosmo’23 for insightful discussions. This work was supported by the Science and Technology Facilities Council (grant numbers ST/T506345/1 and ST/W001225/1). For the purpose of open access, the authors have applied a Creative Commons Attribution (CC-BY) licence to any Author Accepted Manuscript version arising from this work. Supporting research data are available on reasonable request from the corresponding author, Joseph Jackson.

A δN for piece-wise linear model

In this section, we implement the linearised version of the δN approach presented in Sec. 2.4.3, to Starobinsky’s piece-wise linear model discussed in Sec. 3. The first step is to derive the function $N(\phi_{\text{in}}, \dot{\phi}_{\text{in}})$, which returns the number of e-folds realised from the spatially-homogeneous initial field configuration given by ϕ_{in} and $\dot{\phi}_{\text{in}}$ to the end of

inflation. This can be done using the general solution of the Klein–Gordon equation (2.1) with N as the time variable, namely

$$\phi(N) = -\frac{A_{\pm}}{3H^2}N + B_{\pm}^{(1)} + B_{\pm}^{(2)}e^{-3N}. \quad (\text{A.1})$$

The integration constants $B_{\pm}^{(1)}$ and $B_{\pm}^{(2)}$ depend on the initial phase-space coordinates $(\phi_{\text{in}}, \dot{\phi}_{\text{in}})$.

Let us first consider the case where $\phi_{\text{in}} < \phi_{\text{T}}$. By differentiating Eq. (A.1) with respect to time,

$$\dot{\phi} = -\frac{A_-}{3H} - 3HB_-^{(2)}e^{-3N}, \quad (\text{A.2})$$

and combining Eqs. (A.1) and (A.2), one finds

$$N = -\frac{3H^2}{A_-} \left(\phi + \frac{\dot{\phi}}{3H} - B_-^{(1)} + \frac{A_-}{9H^2} \right). \quad (\text{A.3})$$

The constant $B_-^{(1)}$ can be found by requiring that $\phi(0) = \phi_{\text{in}}$ in Eq. (A.1) and $\dot{\phi}(0) = \dot{\phi}_{\text{in}}$ in Eq. (A.2), leading to

$$B_-^{(1)} = \phi_{\text{in}} + \frac{\dot{\phi}_{\text{in}}}{3H} + \frac{A_-}{9H^2}. \quad (\text{A.4})$$

The number of e-folds from $(\phi_{\text{in}}, \dot{\phi}_{\text{in}})$ to the end of inflation at $(\phi_{\text{end}}, \dot{\phi}_{\text{end}})$, is then

$$N_-(\phi_{\text{in}}, \dot{\phi}_{\text{in}}) = \frac{3H^2}{A_-} \left(\phi_{\text{in}} - \phi_{\text{end}} + \frac{\dot{\phi}_{\text{in}} - \dot{\phi}_{\text{end}}}{3H} \right). \quad (\text{A.5})$$

For $\phi_{\text{in}} > \phi_{\text{T}}$, the total number of e-folds can be decomposed into $N_{\text{T}}(\phi_{\text{in}}, \dot{\phi}_{\text{in}})$, the number of e-folds until the transition, and $N_-[\phi_{\text{T}}, \dot{\phi}_{\text{T}}(\phi_{\text{in}}, \dot{\phi}_{\text{in}})]$, the number of e-folds from the transition to the end of inflation. Note that the field velocity at the transition, $\dot{\phi}_{\text{T}}$, is a function of the initial phase-space coordinate $(\phi_{\text{in}}, \dot{\phi}_{\text{in}})$. For $N_{\text{T}}(\phi_{\text{in}}, \dot{\phi}_{\text{in}})$, one can solve Eq. (A.1) for N with $+$ as a subscript and find

$$N_{\text{T}}(\phi_{\text{in}}, \dot{\phi}_{\text{in}}) = \frac{3H^2}{A_+} (B_+^{(1)} - \phi_{\text{T}}) + \frac{1}{3}W_0 \left[\frac{9H^2 B_+^{(2)}}{A_+} e^{-\frac{9H^2}{A_+}(B_+^{(1)} - \phi_{\text{T}})} \right], \quad (\text{A.6})$$

where $W_0(x)$ is the 0th branch of the Lambert function. In this expression, $B_+^{(1)}$ and $B_+^{(2)}$ are set as before by requiring that $\phi(0) = \phi_{\text{in}}$ and $\dot{\phi}(0) = \dot{\phi}_{\text{in}}$ in Eqs. (A.1) and (A.2), leading to

$$B_+^{(1)} = \phi_{\text{in}} + \frac{\dot{\phi}_{\text{in}}}{3H} + \frac{A_+}{9H^2} \quad \text{and} \quad B_+^{(2)} = -\frac{\dot{\phi}_{\text{in}}}{3H} - \frac{A_+}{9H^2}. \quad (\text{A.7})$$

For $N_-[\phi_{\text{T}}, \dot{\phi}_{\text{T}}(\phi_{\text{in}}, \dot{\phi}_{\text{in}})]$, by differentiating Eq. (A.1) with respect to time and evaluating the result at the time $N_{\text{T}}(\phi_{\text{in}}, \dot{\phi}_{\text{in}})$ given in Eq. (A.6), one first finds

$$\dot{\phi}_{\text{T}}(\phi_{\text{in}}, \dot{\phi}_{\text{in}}) = -\frac{A_+}{3H} \left\{ 1 + W_0 \left[\frac{9H^2 B_+^{(2)}}{A_+} e^{-\frac{9H^2}{A_+}(B_+^{(1)} - \phi_{\text{T}})} \right] \right\}. \quad (\text{A.8})$$

Replacing ϕ_{in} by ϕ_{T} and $\dot{\phi}_{\text{in}}$ by the above expression in Eq. (A.5) then gives

$$N_-[\phi_{\text{T}}, \dot{\phi}_{\text{T}}(\phi_{\text{in}}, \dot{\phi}_{\text{in}})] = \frac{3H^2}{A_-} \left(\phi_{\text{T}} - \phi_{\text{end}} - \frac{\dot{\phi}_{\text{end}}}{3H} \right) - \frac{A_+}{3A_-} \left\{ 1 + W_0 \left[\frac{9H^2 B_+^{(2)}}{A_+} e^{-\frac{9H^2}{A_+} (B_+^{(1)} - \phi_{\text{T}})} \right] \right\}. \quad (\text{A.9})$$

Note that the dependence on ϕ_{in} and $\dot{\phi}_{\text{in}}$ is implicit through $B_+^{(1)}$ and $B_+^{(2)}$. One can summarise the above results as

$$N(\phi, \dot{\phi}) = \begin{cases} N_{\text{T}}(\phi, \dot{\phi}) + N_-[\phi_{\text{T}}, \dot{\phi}_{\text{T}}(\phi, \dot{\phi})] & \text{if } \phi \geq \phi_{\text{T}}, \\ N_-(\phi, \dot{\phi}) & \text{if } \phi < \phi_{\text{T}}, \end{cases} \quad (\text{A.10})$$

where $N_{\text{T}}(\phi, \dot{\phi})$, $N_-[\phi_{\text{T}}, \dot{\phi}_{\text{T}}(\phi, \dot{\phi})]$ and $N_-(\phi, \dot{\phi})$ are given above, and where hereafter the subscripts ‘‘in’’ are dropped for convenience.

The next step is to differentiate the number of realised e-folds with respect to the initial field value and its velocity. One obtains

$$\frac{\partial N}{\partial \phi} = \begin{cases} \frac{3H^2}{A_+} \left[1 - \frac{\Delta A}{A_-} \frac{W_0(x)}{1+W_0(x)} \right] & \text{if } \phi \geq \phi_{\text{T}}, \\ \frac{3H^2}{A_-}, & \text{if } \phi < \phi_{\text{T}}, \end{cases} \quad (\text{A.11})$$

and

$$\frac{\partial N}{\partial \dot{\phi}} = \begin{cases} \frac{H}{A_+} \left[1 - \frac{\Delta A}{A_-} \left(1 + \frac{A_+}{9H^2 B_+^{(2)}} \right) \frac{W_0(x)}{1+W_0(x)} \right] & \text{if } \phi \geq \phi_{\text{T}}, \\ \frac{H}{A_-}, & \text{if } \phi < \phi_{\text{T}}, \end{cases} \quad (\text{A.12})$$

where

$$x \equiv \frac{9H^2 B_+^{(2)}}{A_+} e^{-\frac{9H^2}{A_+} (B_+^{(1)} - \phi_{\text{T}})}. \quad (\text{A.13})$$

Then, for a given scale k , one has to evaluate the above derivatives at the time when that scale crosses out the σ -Hubble radius, *i.e.* when $k = \sigma aH$. In the de Sitter limit, this occurs at a time (denoted by a subscript ‘‘*’’ hereafter) $\eta_*(k) = \sigma/k$, or equivalently, $N_*(k) = N_{\text{T}} + \ln[k/(\sigma k_{\text{T}})]$. From Eq. (3.2), one has

$$\phi_*(k) = \begin{cases} -\frac{A_+}{3H^2} \ln\left(\frac{k}{\sigma k_{\text{T}}}\right) + \phi_{\text{T}} & \text{for } k \leq \sigma k_{\text{T}}, \\ -\frac{A_-}{3H^2} \ln\left(\frac{k}{\sigma k_{\text{T}}}\right) + \frac{\Delta A}{9H^2} \left[1 - \left(\frac{k}{\sigma k_{\text{T}}}\right)^{-3} \right] + \phi_{\text{T}} & \text{for } k > \sigma k_{\text{T}}, \end{cases} \quad (\text{A.14})$$

and

$$\dot{\phi}_*(k) = \begin{cases} -\frac{A_+}{3H} & \text{for } k \leq \sigma k_{\text{T}}, \\ -\frac{A_-}{3H} + \frac{\Delta A}{3H} \left(\frac{k}{\sigma k_{\text{T}}}\right)^{-3} & \text{for } k > \sigma k_{\text{T}}. \end{cases} \quad (\text{A.15})$$

For $k \leq \sigma k_{\text{T}}$, one has $\phi_* \geq \phi_{\text{T}}$ and inserting Eqs. (A.14) and (A.15) into Eq. (A.7) leads to $B_{+*}^{(1)} = \phi_{\text{T}} + A_+/(3H^2) \ln(\sigma k_{\text{T}}/k)$ and $B_{+*}^{(2)} = 0$. Therefore, $x_* = 0$ for those scales, and using that $W_0(x) = x + \mathcal{O}(x^2)$, one obtains

$$\left. \frac{\partial N}{\partial \phi} \right|_* = \begin{cases} \frac{3H^2}{A_+} & \text{for } k \leq \sigma k_{\text{T}} \\ \frac{3H^2}{A_-} & \text{for } k > \sigma k_{\text{T}} \end{cases} \quad (\text{A.16})$$

and

$$\left. \frac{\partial N}{\partial \dot{\phi}} \right|_* = \begin{cases} \frac{H}{A_+} \left[1 - \frac{\Delta A}{A_-} \left(\frac{k}{\sigma k_{\text{T}}} \right)^3 \right] & \text{for } k \leq \sigma k_{\text{T}} \\ \frac{H}{A_-} & \text{for } k > \sigma k_{\text{T}} \end{cases}. \quad (\text{A.17})$$

The next step is to evaluate $\delta\phi_k$ and $\delta\dot{\phi}_k$ at the σ -Hubble crossing time, within the full linear cosmological perturbation theory. Recalling that $v = a\delta\phi$ in the spatially-flat gauge, and given that $\mathcal{R} = v/z$ where $z = \text{sign}(\dot{\phi})\sqrt{2a^2\epsilon_1}$, one has

$$\delta\phi_k = -\sqrt{2\epsilon_1}\mathcal{R}_k \quad \text{and} \quad \delta\dot{\phi}_k = -\sqrt{2\epsilon_1} \left(\dot{\mathcal{R}}_k + \frac{\epsilon_2}{2} H\mathcal{R}_k \right). \quad (\text{A.18})$$

For $k \leq \sigma k_{\text{T}}$ (i.e. $\phi_* \geq \phi_{\text{T}}$), from Eqs. (3.3) and (3.4) one has $\epsilon_{1*} = A_+^2/(18H^4)$ while ϵ_{2*} can be discarded, leading to

$$\delta\phi_{k*} = \frac{-A_+}{3H^2}\mathcal{R}_{k*} \quad \text{and} \quad \delta\dot{\phi}_{k*} = \frac{-A_+}{3H^2}\dot{\mathcal{R}}_{k*}. \quad (\text{A.19})$$

For $k > \sigma k_{\text{T}}$ (i.e. $\phi_* < \phi_{\text{T}}$), one obtains

$$\epsilon_{1*} = \frac{A_-^2}{18H^4} \left[1 - \frac{\Delta A}{A_-} \left(\frac{\sigma k_{\text{T}}}{k} \right)^3 \right]^2 \quad \text{and} \quad \epsilon_{2*} = 6 \frac{\frac{\Delta A}{A_-} \left(\frac{\sigma k_{\text{T}}}{k} \right)^3}{1 - \frac{\Delta A}{A_-} \left(\frac{\sigma k_{\text{T}}}{k} \right)^3}, \quad (\text{A.20})$$

leading to

$$\delta\phi_{k*} = \frac{-A_-}{3H^2} \left[1 - \frac{\Delta A}{A_-} \left(\frac{\sigma k_{\text{T}}}{k} \right)^3 \right] \mathcal{R}_{k*} \quad (\text{A.21})$$

and

$$\delta\dot{\phi}_{k*} = -\frac{\Delta A}{H} \left(\frac{\sigma k_{\text{T}}}{k} \right)^3 \mathcal{R}_{k*} - \frac{A_-}{3H^2} \left[1 - \frac{\Delta A}{A_-} \left(\frac{\sigma k_{\text{T}}}{k} \right)^3 \right] \dot{\mathcal{R}}_{k*}. \quad (\text{A.22})$$

Combining the above results into Eq. (2.34), one finally obtains

$$\delta N_k = \begin{cases} -\mathcal{R}_{k*} - \left[1 - \frac{\Delta A}{A_-} \left(\frac{k}{\sigma k_{\text{T}}} \right)^3 \right] \frac{\dot{\mathcal{R}}_{k*}}{3H} & \text{for } k \leq \sigma k_{\text{T}} \\ -\mathcal{R}_{k*} - \left[1 - \frac{\Delta A}{A_-} \left(\frac{k}{\sigma k_{\text{T}}} \right)^{-3} \right] \frac{\dot{\mathcal{R}}_{k*}}{3H} & \text{for } k > \sigma k_{\text{T}} \end{cases}. \quad (\text{A.23})$$

This expression agrees with the one obtained for \hat{C}_k (i.e. the late-time value of $\mathcal{R}_k = -\zeta_k$) in the homogeneous-matching procedure, see Eq. (3.16). This proves that the

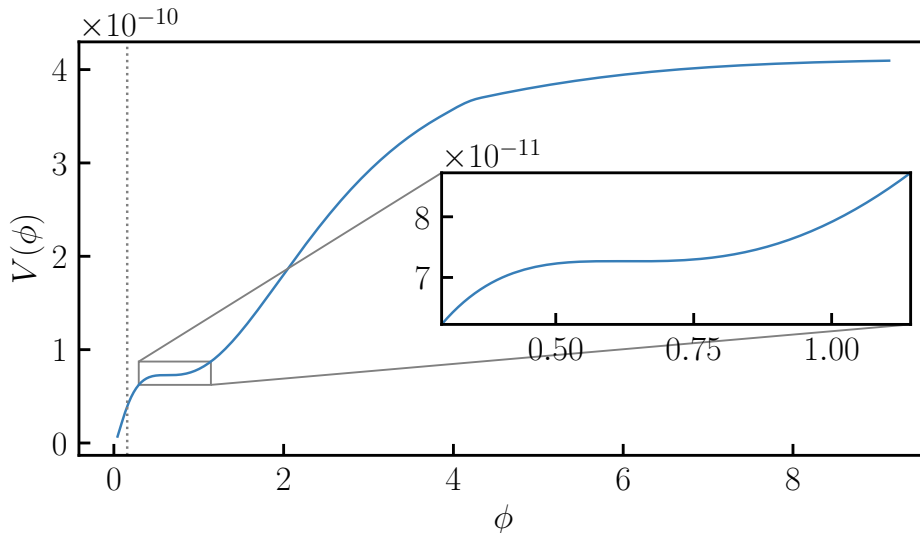


Figure 7. The potential for Higgs inflation modified by quantum corrections [101]. The parameters are chosen such that sufficient PBHs of asteroid mass are produced to provide all of the dark matter, giving the highlighted inflection point. The dotted vertical line is where inflation ends.

homogeneous-matching procedure and the linearised δN formalism are strictly equivalent. This should be clear from the way these two approaches are formulated (namely, they both rely on using linear cosmological perturbation theory below the matching scale and the homogeneous dynamics above that scale), but here the correspondence is shown explicitly in the case of the Starobinsky piece-wise linear potential.

B Example: inflection-point model

A potential with an inflection point can also lead to a phase of ultra-slow-roll inflation and significant PBH production, with many different models proposed, see e.g. [97–100]. Here we will investigate a model motivated by Higgs inflation with quantum corrections [101], which has been used for simulations of stochastic inflation [86, 87]. The potential in Ref. [101] does not have a closed analytical form, but the authors kindly provided numerical data for $V(\phi)$ to reproduce the asteroid mass PBH case, which is plotted in Fig. 7. There is a bump near $\phi = 4$ due to an interpolation, but this has little effect on the dynamics at the inflection point. This model has a phase of ultra-slow roll of ~ 3 e-folds followed by a smooth transition to a constant-roll phase.

Determining the growing and decaying modes can again be done numerically using the homogeneous matching procedure detailed in Eq. (2.27), the result of which is shown in Fig. 8. Both the power spectrum and mode evolution plots show similar behaviour to the Gaussian bump discussed in Sec. 4. Therefore the same conclusions drawn from the Gaussian bump model also apply here. This demonstrates that the dynamics discussed

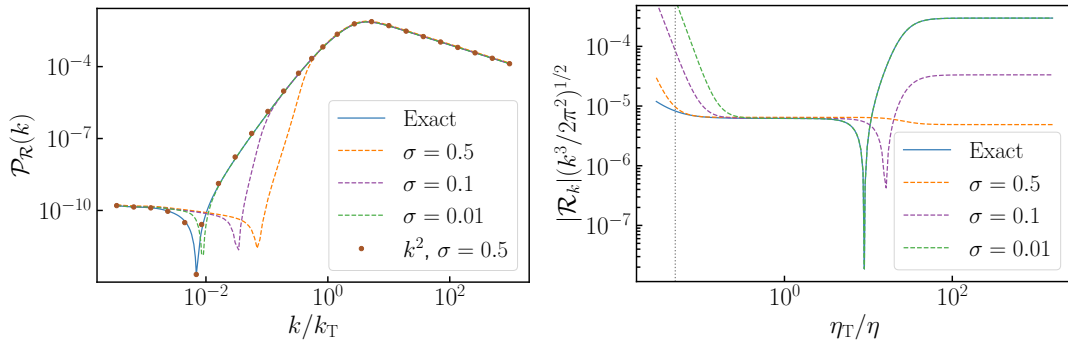


Figure 8. Left: the curvature perturbation power spectrum at the end of inflation for the inflection-point model motivated by Higgs inflation [101]. Right: the evolution of \mathcal{R} for the mode with $k = 0.05k_T$. The solid blue curve is found by numerically solving Eq. (2.4), the dashed curves are found using the numerical matching detailed in Sec. 2.4, and the brown data points are found by including the k^2 correction (2.31). The dotted vertical line is Hubble-exit time. The ultra-slow-roll period ($\epsilon_2 < -3$) starts at $\eta_T = -1/k_T$.

in this paper are a general feature of single-field models with a sudden transition from slow roll to ultra-slow roll, followed by a slow-roll or constant-roll phase to the end of inflation.

C Bessel functions

Let us introduce the parameter

$$\nu^2 = -\frac{\mu^2}{(aH)^2} + \frac{1}{4} = \frac{9}{4} - \epsilon_1 + \frac{3}{2}\epsilon_2 - \frac{1}{2}\epsilon_1\epsilon_2 + \frac{1}{4}\epsilon_2^2 + \frac{1}{2}\epsilon_2\epsilon_3, \quad (\text{C.1})$$

where μ^2 is given in Eq. (2.5). If ν^2 is a constant, then Eq. (2.4) has an exact solution [102]

$$v_k = \sqrt{-\eta}[A_k J_\nu(-k\eta) + B_k Y_\nu(-k\eta)], \quad (\text{C.2})$$

where

$$J_\nu(x) = \left(\frac{x}{2}\right)^\nu \sum_{n=0}^{\infty} \left(\frac{x}{2}\right)^{2n} \frac{(-1)^n}{n!\Gamma(\nu+n+1)} \quad \text{and} \quad Y_\nu(x) = \frac{J_\nu(x) \cos(\nu\pi) - J_{-\nu}(x)}{\sin(\nu\pi)}, \quad (\text{C.3})$$

and Γ is the gamma function. In the standard case the integration constants A_k and B_k are set by using Bunch–Davies initial conditions (2.6). This is the more general form of Eq. (2.19), and reproduces it when $\nu = 3/2$. As both J_ν and Y_ν have power series expansions, the growing and decaying mode interpretation of Eq. (2.14) applies. One can also propagate Eq. (C.2) through the sharp transition of Sec. 3, using Eq. (3.9), to find the post-transition A_k and B_k in an equivalent manner to finding α_k and β_k . While the computation is more complex, one again finds A_k and B_k are different to the

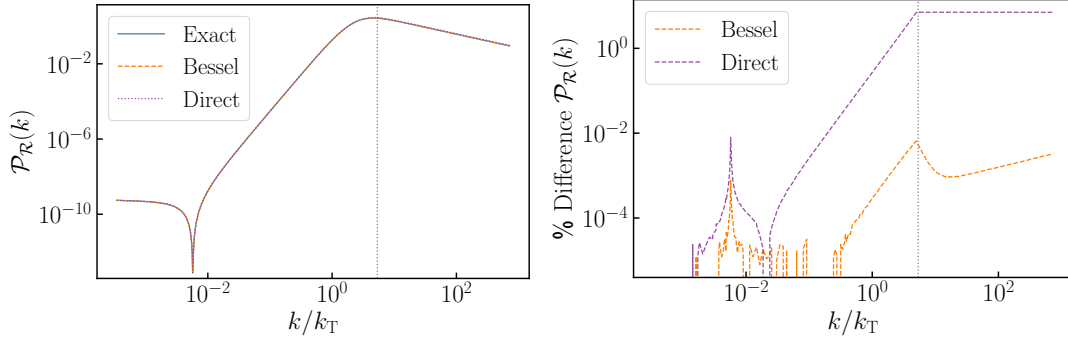


Figure 9. Left panel: the curvature perturbation power spectrum at the end of inflation for a potential with a Gaussian bump (4.1). The solid blue curve is found by numerically solving the full mode equation Eq. (2.4). The orange dashed line uses the intermediate step of finding the homogeneous behaviour using the Bessel functions, see Eqs. (C.5) and (C.6), while the purple dotted line uses the homogeneous matching (2.27) directly. The matching time, η_* , is when ν^2 (C.1) first becomes constant post-transition (for modes to the left of the dotted vertical line), or when $k = 0.5aH$ for modes to the right of the dotted vertical line. Right: the percent difference between the two matching prescriptions and the full numerical result. The ultra-slow-roll period ($\epsilon_2 < -3$) starts at $\eta_{\text{T}} = -1/k_{\text{T}}$.

pre-transition values. This shows the conclusions of Sec. 3 are valid beyond the de Sitter approximation.

The solution given in Eq. (C.2) is valid during any period of constant ν^2 , as is the case during both slow roll and ultra-slow roll. This is true even if following a period when ν^2 is varying, in a piece-wise manner. Then, A_k and B_k can be found by matching onto the full solution for v_k at a time η_* , using

$$\begin{aligned}
 A_k &= \frac{1}{2(-\eta_*)^{3/2}} \frac{2\eta_* Y_\nu(-k\eta_*) v'_{k*} - Y_\nu(-k\eta_*) v_k - 2\eta_* [Y_\nu(-k\eta_*)]' v_{k*}}{J_\nu[Y_\nu(-k\eta_*)]' - Y_\nu(-k\eta_*) [J_\nu(-k\eta_*)]'}, \\
 B_k &= -\frac{1}{2(-\eta_*)^{3/2}} \frac{2\eta_* J_\nu(-k\eta_*) v'_{k*} - J_\nu(-k\eta_*) v_k - 2\eta_* [J_\nu(-k\eta_*)]' v_{k*}}{J_\nu[Y_\nu(-k\eta_*)]' - Y_\nu(-k\eta_*) [J_\nu(-k\eta_*)]'}.
 \end{aligned} \tag{C.4}$$

This allows the homogeneous matching of Sec. 2.4 to be done more accurately with the following steps. Assuming no further sudden transitions occur, then the homogeneous growing and decaying mode coefficients of Eq. (2.12) will be constant until the end of inflation. This is true even if there is a slow variation in ν^2 later. The leading order expansion of Eq. (C.2) can then be used, along with $\mathcal{R} = v_k/z$ and the homogeneous matching (2.27), to give

$$\begin{aligned}
 \hat{C}_k &= \frac{\sqrt{\eta_*}}{z_*} (a_k \eta_*^{-\nu} + b_k \eta_*^\nu) + \\
 & z_* \sqrt{\eta_*} \left\{ a_k \left[\left(\frac{1}{2} - \nu \right) \eta_*^{-1} - \frac{z'}{z} \right] \eta_*^{-\nu} + b_k \left[\left(\frac{1}{2} + \nu \right) \eta_*^{-1} - \frac{z'}{z} \right] \eta_*^\nu \right\} \int_{\eta_*}^0 \frac{d\tilde{\eta}}{z^2(\tilde{\eta})}, \tag{C.5}
 \end{aligned}$$

$$\hat{D}_k = -z_* \sqrt{\eta_*} \left\{ a_k \left[\left(\frac{1}{2} - \nu \right) \eta_*^{-1} - \frac{z'}{z} \right] \eta_*^{-\nu} + b_k \left[\left(\frac{1}{2} + \nu \right) \eta_*^{-1} - \frac{z'}{z} \right] \eta_*^\nu \right\}, \quad (\text{C.6})$$

where

$$\begin{aligned} a_k &= - \left[B_k \frac{\Gamma(\nu)}{\pi} \right] \left(\frac{-k}{2} \right)^{-\nu}, \\ b_k &= \left[\frac{A_k}{\Gamma(\nu+1)} - B_k \frac{\Gamma(-\nu) \cos(\nu\pi)}{\pi} \right] \left(\frac{-k}{2} \right)^\nu. \end{aligned} \quad (\text{C.7})$$

With this approach, any contamination from gradient terms can be effectively removed. This improves the accuracy of the method, and allows the post-transition homogeneous behaviour to be found closer to Hubble exit (corresponding to a matching scale, $k = \sigma aH$, with larger σ).

The method detailed above has been applied numerically in Fig. 9 for the Gaussian bump model, see Sec. 4. The power spectrum at the end of inflation has been reconstructed to test the accuracy of this method against applying Eq. (2.27) directly. For modes which would have left the matching scale ($k = 0.5aH$) before ν^2 becomes constant, the matching has been done at $\eta_* = \eta_T/10$, when ν^2 becomes constant post-transition. The later modes are simply matched when $k = 0.5aH$ (i.e. $\sigma = 0.5$). The dotted line shows when the matching time changes. Using Eqs. (C.5) and (C.6), which effectively removes any gradient terms, produces excellent agreement with the full numerical result. The error is less than 0.01% throughout, while directly applying Eq. (2.27) gives a percent level error. Both have vanishing errors for modes which left the Hubble scale long before the transition.

Periods of constant ν^2 after the slow-roll to ultra-slow-roll transition are present in many models. This is the case for all potentials investigated in this paper, as can be seen, using Eq. (C.1), in Fig. 1. Therefore it is expected that the approach will be applicable in a wide variety of models.

References

- [1] A. A. Starobinsky, *A new type of isotropic cosmological models without singularity*, *Physics Letters B* **91(1)** (1980) 99.
- [2] K. Sato, *First-order phase transition of a vacuum and the expansion of the Universe*, *Monthly Notices of the Royal Astronomical Society* **195(3)** (1981) 467.
- [3] A. H. Guth, *Inflationary universe: A possible solution to the horizon and flatness problems*, *Physical Review D* **23(2)** (1981) 347.
- [4] A. D. Linde, *A new inflationary universe scenario: A possible solution of the horizon, flatness, homogeneity, isotropy and primordial monopole problems*, *Physics Letters B* **108(6)** (1982) 389.
- [5] A. Albrecht and P. J. Steinhardt, *Cosmology for Grand Unified Theories with Radiatively Induced Symmetry Breaking*, *Physical Review Letters* **48(17)** (1982) 1220.
- [6] A. D. Linde, *Chaotic inflation*, *Physics Letters B* **129(3–4)** (1983) 177.

- [7] V. F. Mukhanov and G. V. Chibisov, *Quantum fluctuations and a nonsingular universe*, *Journal of Experimental and Theoretical Physics Letters* **33(10)** (1981) 532.
- [8] V. F. Mukhanov and G. V. Chibisov, *Vacuum energy and large-scale structure of the universe*, *Journal of Experimental and Theoretical Physics* **56(2)** (1982) 258.
- [9] A. A. Starobinsky, *Dynamics of phase transition in the new inflationary universe scenario and generation of perturbations*, *Physics Letters B* **117(3–4)** (1982) 175.
- [10] A. H. Guth and S.-Y. Pi, *Fluctuations in the New Inflationary Universe*, *Physical Review Letters* **49(15)** (1982) 1110.
- [11] S. Hawking, *The development of irregularities in a single bubble inflationary universe*, *Physics Letters B* **115(4)** (1982) 295.
- [12] J. M. Bardeen, P. J. Steinhardt and M. S. Turner, *Spontaneous creation of almost scale-free density perturbations in an inflationary universe*, *Physical Review D* **28(4)** (1983) 679.
- [13] D. H. Lyth and A. R. Liddle, *The Primordial Density Perturbation: Cosmology, Inflation and the Origin of Structure*, Cambridge University Press (2009).
- [14] D. Baumann, *Cosmology*, Cambridge University Press (2022).
- [15] PLANCK COLLABORATION, *Planck 2015 results. XIII. Cosmological parameters*, *Astronomy & Astrophysics* **594** (2016) A13 [[1502.01589](#)].
- [16] PLANCK COLLABORATION, *Planck 2015 results. XX. Constraints on inflation*, *Astronomy & Astrophysics* **594** (2016) A20 [[1502.02114](#)].
- [17] PLANCK COLLABORATION, *Planck 2018 results. VI. Cosmological parameters*, *Astronomy & Astrophysics* **641** (2020) A6 [[1807.06209](#)].
- [18] J. Chluba, J. Hamann and S. P. Patil, *Features and new physical scales in primordial observables: Theory and observation*, *International Journal of Modern Physics D* **24(10)** (2015) 1530023 [[1505.01834](#)].
- [19] C. Caprini and D. G. Figueroa, *Cosmological backgrounds of gravitational waves*, *Classical and Quantum Gravity* **35(16)** (2018) 163001 [[1801.04268](#)].
- [20] G. Domenech, *Scalar Induced Gravitational Waves Review*, *Universe* **7(11)** (2021) 398 [[2109.01398](#)].
- [21] O. Özsoy and G. Tasinato, *Inflation and Primordial Black Holes*, *Universe* **9(5)** (2023) 203 [[2301.03600](#)].
- [22] NANOGrav COLLABORATION, *The NANOGrav 15 yr Data Set: Evidence for a Gravitational-wave Background*, *The Astrophysical Journal Letters* **951(1)** (2023) L8 [[2306.16213](#)].
- [23] EPTA COLLABORATION AND INPTA COLLABORATION, *The second data release from the European Pulsar Timing Array III. Search for gravitational wave signals*, *Astronomy & Astrophysics* **678** (2023) A50 [[2306.16214](#)].
- [24] H. Xu et al., *Searching for the Nano-Hertz Stochastic Gravitational Wave Background with the Chinese Pulsar Timing Array Data Release I*, *Research in Astronomy and Astrophysics* **23(7)** (2023) 075024 [[2306.16216](#)].
- [25] NANOGrav COLLABORATION, *The NANOGrav 15 yr Data Set: Search for Signals from New Physics*, *The Astrophysical Journal Letters* **951(1)** (2023) L11 [[2306.16219](#)].

- [26] B. Carr, F. Kühnel and M. Sandstad, *Primordial black holes as dark matter*, *Physical Review D* **94(8)** (2016) 083504 [[1607.06077](#)].
- [27] B. Carr, K. Kohri, Y. Sendouda and J. Yokoyama, *Constraints on primordial black holes*, *Reports on Progress in Physics* **84(11)** (2021) 116902 [[2002.12778](#)].
- [28] B. Carr and F. Kühnel, *Primordial Black Holes as Dark Matter: Recent Developments*, *Annual Review of Nuclear and Particle Science* **70** (2020) 355 [[2006.02838](#)].
- [29] A. M. Green and B. J. Kavanagh, *Primordial black holes as a dark matter candidate*, *Journal of Physics G* **48(4)** (2021) 043001 [[2007.10722](#)].
- [30] C. T. Byrnes, P. S. Cole and S. P. Patil, *Steepest growth of the power spectrum and primordial black holes*, *Journal of Cosmology and Astroparticle Physics* **2019(06)** (2019) 028 [[1811.11158](#)].
- [31] P. S. Cole, A. D. Gow, C. T. Byrnes and S. P. Patil, *Steepest growth re-examined: repercussions for primordial black hole formation*, (2022) [[2204.07573](#)].
- [32] A. Karam *et al.*, *Anatomy of single-field inflationary models for primordial black holes*, *Journal of Cosmology and Astroparticle Physics* **2023(03)** (2023) 013 [[2205.13540](#)].
- [33] M. Sasaki, *Large Scale Quantum Fluctuations in the Inflationary Universe*, *Progress of Theoretical Physics* **76(5)** (1986) 1036.
- [34] V. F. Mukhanov, *Quantum theory of gauge-invariant cosmological perturbations*, *Journal of Experimental and Theoretical Physics* **67(7)** (1988) 1297.
- [35] J. Kristiano and J. Yokoyama, *Ruling Out Primordial Black Hole Formation From Single-Field Inflation*, (2022) [[2211.03395](#)].
- [36] A. Ota, M. Sasaki and Y. Wang, *Scale-invariant enhancement of gravitational waves during inflation*, *Modern Physical Letters A* **38(12n13)** (2023) 2350063 [[2209.02272](#)].
- [37] S. Choudhury, M. R. Gangopadhyay and M. Sami, *No-go for the formation of heavy mass Primordial Black Holes in Single Field Inflation*, (2023) [[2301.10000](#)].
- [38] H. Motohashi and Y. Tada, *Squeezed bispectrum and one-loop corrections in transient constant-roll inflation*, *Journal of Cosmology and Astroparticle Physics* **2023(08)** (2023) 069 [[2303.16035](#)].
- [39] H. Firouzjahi and A. Riotto, *Primordial Black Holes and Loops in Single-Field Inflation*, (2023) [[2304.07801](#)].
- [40] G. Franciolini, A. J. Iovino, M. Taoso and A. Urbano, *One loop to rule them all: Perturbativity in the presence of ultra slow-roll dynamics*, (2023) [[2305.03491](#)].
- [41] J. Fumagalli *et al.*, *One-loop infrared rescattering by enhanced scalar fluctuations during inflation*, (2023) [[2307.08358](#)].
- [42] J. Fumagalli, *Absence of one-loop effects on large scales from small scales in non-slow-roll dynamics*, (2023) [[2305.19263](#)].
- [43] Y. Tada, T. Terada and J. Tokuda, *Cancellation of quantum corrections on the soft curvature perturbations*, (2023) [[2308.04732](#)].
- [44] A. A. Starobinskii, *Multicomponent de Sitter (inflationary) stages and the generation of perturbations*, *Journal of Experimental and Theoretical Physics Letters* **42(3)** (1985) 152.

- [45] M. Sasaki and E. D. Stewart, *A General Analytic Formula for the Spectral Index of the Density Perturbations Produced during Inflation*, *Progress of Theoretical Physics* **95(1)** (1996) 71 [[astro-ph/9507001](#)].
- [46] M. Sasaki and T. Tanaka, *Super-Horizon Scale Dynamics of Multi-Scalar Inflation*, *Progress of Theoretical Physics* **99(5)** (1998) 763 [[gr-qc/9801017](#)].
- [47] D. H. Lyth, K. A. Malik and M. Sasaki, *A general proof of the conservation of the curvature perturbation*, *Journal of Cosmology and Astroparticle Physics* **2005(05)** (2005) 004 [[astro-ph/0411220](#)].
- [48] D. Wands, K. A. Malik, D. H. Lyth and A. R. Liddle, *New approach to the evolution of cosmological perturbations on large scales*, *Physical Review D* **62(4)** (2000) 043527 [[astro-ph/0003278](#)].
- [49] D. H. Lyth and D. Wands, *Conserved cosmological perturbations*, *Physical Review D* **68(10)** (2003) 103515 [[astro-ph/0306498](#)].
- [50] D. H. Lyth and Y. Rodriguez, *Inflationary Prediction for Primordial Non-Gaussianity*, *Physical Review Letters* **95(12)** (2005) 121302 [[astro-ph/0504045](#)].
- [51] D. Artigas, J. Grain and V. Vennin, *Hamiltonian formalism for cosmological perturbations: the separate-universe approach*, *Journal of Cosmology and Astroparticle Physics* **2022(02)** (2022) 001 [[2110.11720](#)].
- [52] D. S. Salopek and J. R. Bond, *Nonlinear evolution of long-wavelength metric fluctuations in inflationary models*, *Physical Review D* **42(12)** (1990) 3936.
- [53] G. I. Rigopoulos and E. P. S. Shellard, *Separate universe approach and the evolution of nonlinear superhorizon cosmological perturbations*, *Physical Review D* **68(12)** (2003) 123518 [[astro-ph/0306620](#)].
- [54] M. Biagetti, G. Franciolini, A. Kehagias and A. Riotto, *Primordial black holes from inflation and quantum diffusion*, *Journal of Cosmology and Astroparticle Physics* **2018(07)** (2018) 032 [[1804.07124](#)].
- [55] H. Firouzjahi, A. Nassiri-Rad and M. Noorbala, *Stochastic nonattractor inflation*, *Physical Review D* **102(12)** (2020) 123504 [[2009.04680](#)].
- [56] Y.-F. Cai *et al.*, *Highly non-Gaussian tails and primordial black holes from single-field inflation*, *Journal of Cosmology and Astroparticle Physics* **2022(12)** (2022) 034 [[2207.11910](#)].
- [57] S. Pi and M. Sasaki, *Logarithmic Duality of the Curvature Perturbation*, *Physical Review Letters* **131(1)** (2023) 011002 [[2211.13932](#)].
- [58] S. Hooshangi, M. H. Namjoo and M. Noorbala, *Tail diversity from inflation*, (2023) [[2305.19257](#)].
- [59] K. Enqvist, S. Nurmi, D. Podolsky and G. I. Rigopoulos, *On the divergences of inflationary superhorizon perturbations*, *Journal of Cosmology and Astroparticle Physics* **2008(04)** (2008) 025 [[0802.0395](#)].
- [60] T. Fujita, M. Kawasaki, Y. Tada and T. Takesako, *A new algorithm for calculating the curvature perturbations in stochastic inflation*, *Journal of Cosmology and Astroparticle Physics* **2013(12)** (2013) 036 [[1308.4754](#)].

- [61] V. Vennin and A. A. Starobinsky, *Correlation functions in stochastic inflation*, *The European Physical Journal C* **75** (2015) 413 [[1506.04732](#)].
- [62] S. M. Leach, M. Sasaki, D. Wands and A. R. Liddle, *Enhancement of superhorizon scale inflationary curvature perturbations*, *Physical Review D* **64**(2) (2001) 023512 [[astro-ph/0101406](#)].
- [63] A. A. Starobinskii, *Spectrum of adiabatic perturbations in the universe when there are singularities in the inflation potential*, *Journal of Experimental and Theoretical Physics Letters* **55**(9) (1992) 489.
- [64] D. J. Schwarz, C. A. Terrero-Escalante and A. A. García, *Higher order corrections to primordial spectra from cosmological inflation*, *Physics Letters B* **517**(3–4) (2001) 243 [[astro-ph/0106020](#)].
- [65] S. M. Leach, A. R. Liddle, J. Martin and D. J. Schwarz, *Cosmological parameter estimation and the inflationary cosmology*, *Physical Review D* **66**(2) (2002) 023515 [[astro-ph/0202094](#)].
- [66] K. Dimopoulos, *Ultra slow-roll inflation demystified*, *Physics Letters B* **775** (2017) 262 [[1707.05644](#)].
- [67] C. Pattison, V. Vennin, H. Assadullahi and D. Wands, *The attractive behaviour of ultra-slow-roll inflation*, *Journal of Cosmology and Astroparticle Physics* **2018**(08) (2018) 048 [[1806.09553](#)].
- [68] K. A. Malik and D. Wands, *Cosmological perturbations*, *Physics Reports* **475**(1–4) (2009) 1 [[0809.4944](#)].
- [69] S. Weinberg, *Adiabatic modes in cosmology*, *Physical Review D* **67**(12) (2003) 123504 [[astro-ph/0302326](#)].
- [70] L. Kofman, A. Linde and A. A. Starobinsky, *Reheating after inflation*, *Physical Review Letters* **73**(24) (1994) 3195 [[hep-th/9405187](#)].
- [71] B. A. Bassett, S. Tsujikawa and D. Wands, *Inflation dynamics and reheating*, *Reviews of Modern Physics* **78**(2) (2006) 537 [[astro-ph/0507632](#)].
- [72] C. Gordon, D. Wands, B. A. Bassett and R. Maartens, *Adiabatic and entropy perturbations from inflation*, *Physical Review D* **63**(2) (2001) 023506 [[astro-ph/0009131](#)].
- [73] A. E. Romano, S. Mooij and M. Sasaki, *Adiabaticity and gravity theory independent conservation laws for cosmological perturbations*, *Physics Letters B* **755** (2016) 464 [[1512.05757](#)].
- [74] C. Pattison, V. Vennin, H. Assadullahi and D. Wands, *Stochastic inflation beyond slow roll*, *Journal of Cosmology and Astroparticle Physics* **2019**(07) (2019) 031 [[1905.06300](#)].
- [75] D. Wands, *Duality invariance of cosmological perturbation spectra*, *Physical Review D* **60**(2) (1999) 023507 [[gr-qc/9809062](#)].
- [76] J. Martin and L. Sriramkumar, *The scalar bi-spectrum in the Starobinsky model: The equilateral case*, *Journal of Cosmology and Astroparticle Physics* **2012**(01) (2012) 008 [[1109.5838](#)].
- [77] J. Martin, L. Sriramkumar and D. K. Hazra, *Sharp inflaton potentials and bi-spectra:*

- effects of smoothening the discontinuity, *Journal of Cosmology and Astroparticle Physics* **2014(09)** (2014) 039 [[1404.6093](#)].
- [78] N. Ahmadi *et al.*, Quantum diffusion in sharp transition to non-slow-roll phase, *Journal of Cosmology and Astroparticle Physics* **2022(08)** (2022) 078 [[2207.10578](#)].
- [79] S. Pi and J. Wang, Primordial black hole formation in Starobinsky's linear potential model, *Journal of Cosmology and Astroparticle Physics* **2023(06)** (2023) 018 [[2209.14183](#)].
- [80] P. Carrilho, K. A. Malik and D. J. Mulryne, Dissecting the growth of the power spectrum for primordial black holes, *Physical Review D* **100(10)** (2019) 103529 [[1907.05237](#)].
- [81] S. S. Mishra and V. Sahni, Primordial black holes from a tiny bump/dip in the inflaton potential, *Journal of Cosmology and Astroparticle Physics* **2020(04)** (2020) 007 [[1911.00057](#)].
- [82] P. S. Cole, A. D. Gow, C. T. Byrnes and S. P. Patil, Primordial black holes from single-field inflation: a fine-tuning audit, *Journal of Cosmology and Astroparticle Physics* **2023(08)** (2023) 031 [[2304.01997](#)].
- [83] A. A. Starobinsky, *Stochastic De Sitter (Inflationary) Stage in the Early Universe*, in *Lecture Notes in Physics (Field Theory, Quantum Gravity and Strings)*, vol. 246, p. 107, 1988.
- [84] A. A. Starobinsky and J. Yokoyama, Equilibrium state of a self-interacting scalar field in the de Sitter background, *Physical Review D* **50(10)** (1994) 6357 [[astro-ph/9407016](#)].
- [85] A. De and R. Mahbub, Numerically modeling stochastic inflation in slow-roll and beyond, *Physical Review D* **102(12)** (2020) 123509 [[2010.12685](#)].
- [86] D. G. Figueroa, S. Raatikainen, S. Räsänen and E. Tomberg, Non-Gaussian Tail of the Curvature Perturbation in Stochastic Ultraslow-Roll Inflation: Implications for Primordial Black Hole Production, *Physical Review Letters* **127(10)** (2021) 101302 [[2012.06551](#)].
- [87] D. G. Figueroa, S. Raatikainen, S. Räsänen and E. Tomberg, Implications of stochastic effects for primordial black hole production in ultra-slow-roll inflation, *Journal of Cosmology and Astroparticle Physics* **2022(05)** (2022) 027 [[2111.07437](#)].
- [88] S. S. Mishra, E. J. Copeland and A. M. Green, Primordial black holes and stochastic inflation beyond slow roll: I – noise matrix elements, (2023) [[2303.17375](#)].
- [89] D. Polarski and A. A. Starobinsky, Semiclassicality and decoherence of cosmological perturbations, *Classical and Quantum Gravity* **13(3)** (1996) 377 [[gr-qc/9504030](#)].
- [90] J. Lesgourgues, D. Polarski and Starobinsky, Quantum-to-classical transition of cosmological perturbations for non-vacuum initial states, *Nuclear Physics B* **497(1–2)** (1997) 479 [[gr-qc/9611019](#)].
- [91] C. Kiefer and D. Polarski, Why do Cosmological Perturbations Look Classical to Us?, *Advanced Science Letters* **2(2)** (2009) 164 [[0810.0087](#)].
- [92] J. Martin and V. Vennin, Quantum discord of cosmic inflation: Can we show that CMB anisotropies are of quantum-mechanical origin?, *Physical Review D* **93(2)** (2016) 023505 [[1510.04038](#)].

- [93] J. Martin and V. Vennin, *Obstructions to Bell CMB experiments*, *Physical Review D* **96(6)** (2017) 063501 [[1706.05001](#)].
- [94] J. Martin, A. Micheli and V. Vennin, *Discord and decoherence*, *Journal of Cosmology and Astroparticle Physics* **2022(04)** (2022) 051 [[2112.05037](#)].
- [95] D. Cruces, C. Germani and T. Prokopec, *Failure of the stochastic approach to inflation beyond slow-roll*, *Journal of Cosmology and Astroparticle Physics* **2019(03)** (2019) 048 [[1807.09057](#)].
- [96] G. Domènech, G. Vargas and T. Vargas, *An exact model for enhancing/suppressing primordial fluctuations*, (2023) [[2309.05750](#)].
- [97] J. García-Bellido and E. Ruiz Morales, *Primordial black holes from single field models of inflation*, *Physics of the Dark Universe* **18** (2017) 47 [[1702.03901](#)].
- [98] H. Di and Y. Gong, *Primordial black holes and second order gravitational waves from ultra-slow-roll inflation*, *Journal of Cosmology and Astroparticle Physics* **2018(07)** (2018) 007 [[1707.09578](#)].
- [99] G. Ballesteros and M. Taoso, *Primordial black hole dark matter from single field inflation*, *Physical Review D* **97(2)** (2018) 023501 [[1709.05565](#)].
- [100] S. R. Geller, W. Qin, E. McDonough and D. I. Kaiser, *Primordial black holes from multifield inflation with nonminimal couplings*, *Physical Review D* **106(6)** (2022) 063535 [[2205.04471](#)].
- [101] S. Räsänen and E. Tomberg, *Planck scale black hole dark matter from Higgs inflation*, *Journal of Cosmology and Astroparticle Physics* **2019(01)** (2019) 038 [[1810.12608](#)].
- [102] E. D. Stewart and D. H. Lyth, *A more accurate analytic calculation of the spectrum of cosmological perturbations produced during inflation*, *Physics Letters B* **302(2–3)** (1993) 171 [[gr-qc/9302019](#)].